FRACTURE NETWORK CHARACTERIZATION OF SYN-TECTONIC YOUNGER GRANITE, WESTERN DHARWAR CRATON (SOUTH INDIA)

Thesis submitted towards partial fulfillment
of
Master of Science degree
in
Applied Geology

by
Arka Pratim Chatterjee

Under the supervision of

Dr. Tridib Kumar Mondal

DEPARTMENT OF GEOLOGICAL SCIENCES
JADAVPUR UNIVERSITY, KOLKATA

May, 2019

Dedicated to my family members

যাদবপুর বিশ্ববিদ্যালয়
কলকাতা-৭০০০৩২, ভারত

JADAVPUR UNIVERSITY
KOLKATA-700032, INDIA

FACULTY OF SCIENCE : DEPARTMENT OF GEOLOGICAL SCIENCES

CERTIFICATE

This is to certify that **Mr. Arka Pratim Chatterjee, (Registration number: 128272 of 2014-15, Class roll no. 001720402005)** an M. Sc. Final Year student of the Department of Geological Sciences, Jadavpur University worked under my guidance and completed the thesis entitled **"FRACTURE NETWORK CHARACTERIZATION OF SYN-TECTONIC YOUNGER GRANITE, DHARWAR CRATON (SOUTH INDIA)"** for partial fulfillment of the M.Sc. Final examination 2019 in Applied Geology of the Faculty of Science, Jadavpur University, Kolkata.

Mr. Chatterjee has fulfilled all the prescribed requirements and this work has not been presented for any degree or diploma elsewhere.

Supervisor
Dr. Tridib Kumar Mondal
Assistant Professor,
Department of Geological Sciences,
Jadavpur University.
Date: 30.5.19

Dr. Tridib Kumar Mondal
Assistant Professor
Department of Geological Sciences
Jadavpur University
Kolkata - 700 032, India

30.05.2019

Head
Department of Geological Sciences
Date:

Head
Department of Geological Sciences
Jadavpur University
Kolkata-700032

দূরভাষ : ২৪১৪-৬৬৬৬/প্রসারণ : ২২৬৮ Website : www.jadavpur.edu Phone : 2414 6666/Extn. 2268
E-mail : hod_geological@jdvu.ac.in

ACKNOWLEDGEMENT

I would like to convey my deepest gratitude to my family members for their constant love, support and encouragement that they have showered upon me.

I express my gratitude and my sincere thanks to my supervisor, Dr. Tridib Kumar Mondal for his guidance and motivation during the entire duration of my thesis work.

I convey my thanks and gratitude to Prof. Sanjoy Sanyal, Head of the Department of Geological sciences, for making available all departmental facilities during my study period. A partial financial support of this project was made by the University.

I also express my gratitude to the American Geophysical Union (AGU), for selecting me to be a presenter at the e-Lightning session at the Fall Meeting 2018, in Washington D.C. and also to AGU Tectonophysics Section Board for selecting me to be a Student Travel Grant awardee.

I would like to express my sincere gratitude to my seniors Mr. Sankha Subhra Acharyya and Mr. Dip Das and also to my batch mate Mr. Rajdeep Mondal, for discussions during the initiation of this project. I would also like to acknowledge Ms. Sreyashi Bhowmick, Mr. Subha Saha and Mr. Ayan Patsa for their help during field work.

Dr. Dave Healy, University of Aberdeen, deserves special mention for helping out with issues I had while using FracPaQ. Comments and suggestions provided by Prof. Tom Blenkinsop, Dr. Bjarne Almqvist, Dr. Nicholas Guy and Mr. Mayukh Talukdar at AGU 2018, have also proved very useful.

Finally I take this opportunity to acknowledge the love, friendship and help rendered by all my friends, seniors and juniors in Jadavpur University, without whom the experience would have been much less memorable.

Arka Pratim Chatterjee

ABSTRACT

The study of fracture network system in granite has great implications in understanding the regional tectonics and also help to apprehend how fractures develop in them. It is known that the study of branches and nodes of fracture network can be useful to define the geometrical features of any fracture system. In the present study, this approach is followed to analyze the fracture network from the 2.61 Ga Chitradurga granite (CDG) of Archaean lode-gold bearing Chitradurga Schist Belt (Dharwar Craton, south India). The CDG is known to have emplaced during regional deformation, and the fabric in Northern part of the granite is simple shear dominated, while Southern part of it is pure shear dominated. This granitic pluton is oriented NNW-SSE, so that the Northern portion is closer to the Chitradurga Shear Zone (CSZ) than Southern portion. It is also replete with crisscross fractures with various orientations. The present investigation is aimed at understanding how this fracture network occurs and varies from pure shear to simple shear dominated regions in CDG. From topological analysis, it is observed that the total dimensionless intensity of fractures in northern part of the CDG is twice as much as the southern part. It is also noted that the proportion of isolated (I), abutting (Y), and crosscutting (X) nodes in northern and southern parts of the CDG are found to be 8.17, 3.29 and 5.56 respectively. Further, the average numbers of connections per branch (C_B) are calculated to be 1.78 and 1.88 for northern and southern parts of CDG respectively. Similar contrasting results of average number of connections per line (C_L) were obtained; which points to the ability of network topology to successfully quantify the differences between fracture networks formed in the same sample space, under different stress conditions. So it is envisaged that the pre-existing fabric along with regional far-field stresses in the CDG played an important role in partitioning the strain and subsequently developing the fracture network in them and this study establishes the credibility of using topology as a reliable tool to quantify and analyze differences between disparate fracture networks.

Key words: Chitradurga granite, Fracture network, Network Topology, Node and branch analysis, Dharwar craton, South India

CONTENTS

LIST OF FIGURES

LIST OF TABLES

CHAPTER 1

Introduction

1.1 General

Fractures are a ubiquitous feature of upper crustal rocks and are equally useful in determining the physical property of a rock body compared to the grain scale textural features. Furthermore, the study of fractures on a regional scale allows us to reconstruct the brittle tectonics of the region, reflecting upon the prevalent paleostress conditions. From an economic perspective, fractures are pathways for upper crustal fluid flow, and their study opens up new exploration strategies for hydrothermal mineral deposits.

In this study, fracture networks belonging to exposed outcrops of Chitradurga Granite, adjacent to Chitradurga Shear Zone (CSZ), an Archean Greenstone Belt in South India, are subjected to two dimensional topological analysis. Most of the previous studies regarding fractures have

followed conventional methods of paleostress analysis to draw conclusions by interpreting results. This work aims to open up a new dimension of study of fractures through the lens of topology, increasing our understanding of how fractures behave and grow to form networks under particular states of stress.

Definition of a fracture network

Fractures are discreet discontinuities in the Earth's crust, forming planes of predominantly brittle deformation, very narrow local aperture compared to the lateral extents along the other two dimensions, along which, the surrounding rock mass does not show any sign of relative displacement. Fractures can form as a result of external or internal stress, such as tectonic forces and thermal or residual stress, respectively. Depending on the orientation of maximum, intermediate and minimum stress directions in three dimensions, fractures can be of three broad categories: Mode I (extensional), where displacement is perpendicular to the opening direction of the fracture, Mode II (sliding), where displacement takes by shear perpendicular to the edge and Mode III (tearing) which involves slip parallel to the edge of the crack. Fractures can also exist in mixed mode category.

A fracture network can be regarded as a system of fractures developed within the same rock volume. A network may involve a number of distinct fracture sets, which may or may not intersect. They generally evolve over time and vary in their spatial distribution. The individual fractures can be described by their geometrical attributes such as orientation, size, morphology, length, angle etc. or by other forms of classification such as fracture type, mineral fill etc.

Fracture sets can be characterized by their statistical distribution of these attributes, such as averages or ranges. The geometry of the fractures is established by measurement, involving the spatial orientation of the fracture surface, together with some physical dimension, such as trace length, area or volume. So in time, a growing system of fractures will interact with each other and the rock matrix, to control the physics of the rock. Hence, not only is the individual fracture geometry a controlling factor of the bulk rock property, but also the interactive relationships between individual fractures and fracture sets. This interaction is studied by a scale invariant mathematical tool known as 'topology'.

1.2 Objectives

The primary objectives of this study are as follows:

i) To create detailed digitized maps of fractured outcrops of Chitradurga Granite

ii) To quantify and characterize these fracture networks with the help of node and branch topology

iii) Determining the variation of topological features along the length of the pluton as well as a function of spatial variation from the Chitradurga Shear Zone (CSZ)

iv) To find out the role of pre-existing fractures (thermal) in the development of present fracture network.

1.3 Methodology

A two pronged approach was taken to tackle this project. We needed to collect the available data from the outcrops, digitize them and feed the files into a tool which would analyse them to give us results which would be interpreted as per our requirements. The following approaches were used:

- **Fieldwork**: Involved taking 2D digital images of horizontal outcrops of Chitradurga Granite and measuring the attitudes of fracture planes inside the granite where possible.
- **Laboratory work**: Where the photographs were digitized using CorelDraw® and the fracture length traces were used as input files for the MATLAB based code FracPaQ, used to analyse the data and obtain results.

1.4 Layout

The following chapters are systematically arranged to introduce the reader to the setting of the study area and the research problem. **Chapter 2** consists of a brief but acute description of the regional geology of the studied area and accounts some of the previous work that has been performed in the Dharwar Craton of South India. **Chapter 3** gives an overview of the principles behind network topology used for the analysis. **Chapter 4** is a walkthrough of the process by which the present study was conducted. **Chapter 5** presents some discussions or inferences

this study points towards. It also contains concluding remarks and points towards further research.

CHAPTER 2

Regional Geology of the study area (Chitradurga granite)

2.1 Introduction

The present study comprises the application of network topology to study the characteristics of fractures in the Chitradurga granite, which is associated with the Chitradurga-Gadag suberbelt, also called the Chitradurga Schist Belt, situated in between the Eastern and Western Dharwar cratons.

The Chitradurga Schist belt is NW-SE trending, Archean age Greenstone belt of Western Dharwar craton (WDC), South India (Chakrabarti et al., 2006). It comprises of thick volcano sedimentary unit which is metamorphosed up to greeschist to lower amphibolite facies. Earlier literature studies on schist belt have been concentrated on the broad lithological and

geochemical investigation (Beeraiah et al. 1998 and Chadwick et al., 2003; Chakrabarti et al., 2006). The study on late-stage brittle deformation of (such as fractures and faults) of Chitradurga Schist Belt in light of regional tectonics has been limited to fault-slip analysis and magnetic fabric studies. Hence the need arose to conduct a comprehensive study of the fractures of the Chitradurga Granite, associated with the CSZ, in light of regional tectonics. However, before going into details of Chitradurga Schist Belt, it is important to know about the regional geology and previous studies of the rocks of this region.

2.2 Regional Geology

The Indian craton consists Precambrian terrains and mobile belts (Fig. 2.1) that comprises low to high-grade crystalline rocks. These Precambrian terrains consist of continental crust and are known as cratons (Sharma, 2009). The southern Indian shield consists of two major units- Dharwar craton in the north and Southern Granulite Terrain (SGT) in the south (Naqvi and Rogers, 1987; Chakrabarti

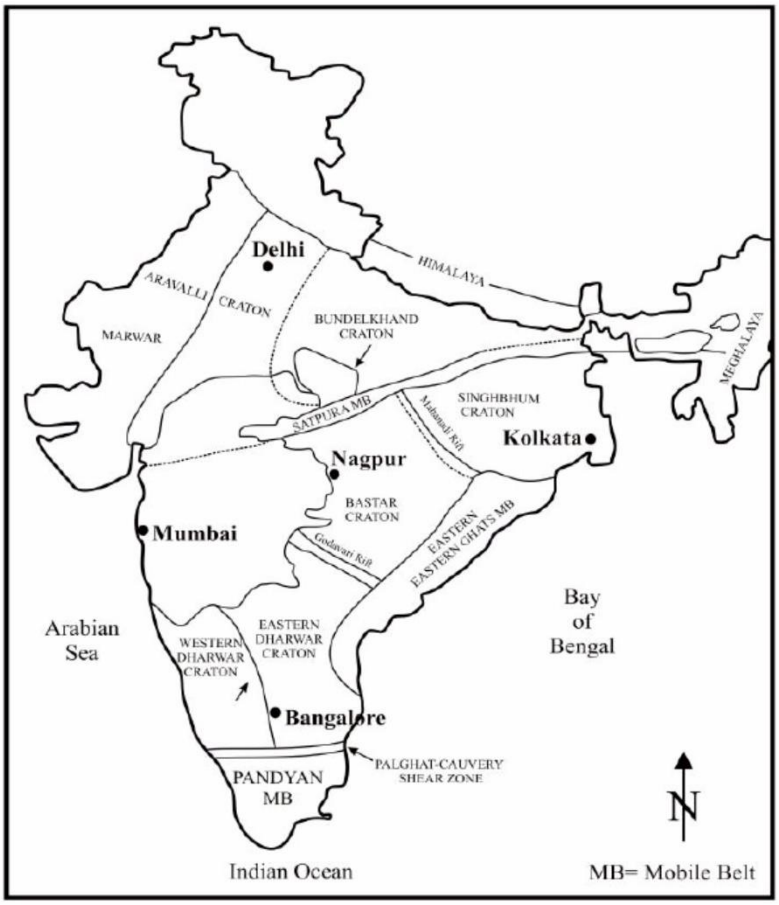

Fig 2.1: The map shows the cratons and mobile belts (MB) in India (after Ramakrishnan and Vaidyanadhan, 2010). Black arrow in the western Dharwar craton demarks the study area.

et al., 2006). The Dharwar province exhibits granite-greenstone terrain mainly characterized by several NW-SE to NNW-SSE trending schistose rocks. The SGT is mainly characterized by

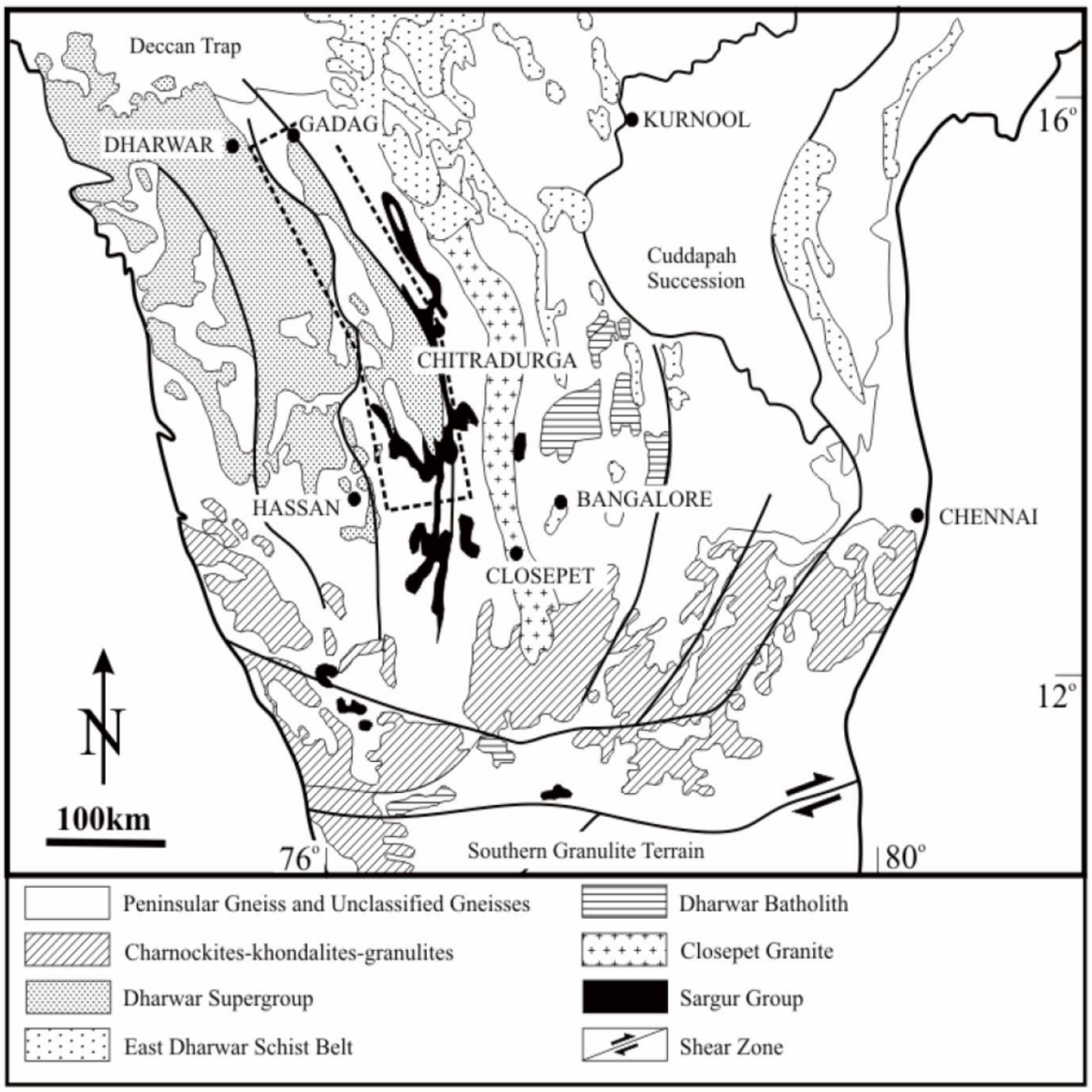

Fig. 2.2 Regional geological map of Dharwar Craton (after Valdiya, 2010). Dashed box represents the Chitradurga Schist Belt.

Western Dharwar Craton (WDC)	Eastern Dharwar Craton (EDC)
1. Dharwar schist belts - large with volcanic, subordinate sediments	1. Dharwar green stone belts -narrow, with dominant pillowed basalts
2. Peninsular Gneiss (>3000 Ma) basement having angular unconformity with the Dharwar. Basement gneiss inliers within schist belt	2. Dharwar batholoth (2500 - 2700 Ma) intusive on all sides. Diapiric gneiss domes are common
3. Three fold succession of: (i) Basalt - arenite-BIF, (ii) Shelf facies at the margin and homotaxial pillowed basalt-BIF in deeper waters, (iii) Greywackes-BIF-volcanics	3. Three folds succession of: (i) Rare shelf sediments disrupted into screens at the belt margins, (ii) Pillowed volcanic, greywackes BIF, (iii) Felsic volcanic , volcanogenic conglomerate ('Champion Gneiss')
4. Older sequence (Sargur Group) as narrow belts and enclaves, abundant in the south	4. Older sequence (Warangal group) mostly as enclaves in the north east; and Salem Group (?) in the south
5. Intermediate pressure (kyanite - sillimanite type) metamorphism	5. Low pressure (andalusite -sillimanite type) metamorphism

Table 2.1 Difference between western Dharwar craton (WDC) and eastern Dharwar craton (EDC) (after Ramakrishnan, 1994; Ramakrishnan and Vaidyanandhan, 2010).

charnockites, mafic granulites and khondalites which are intersected by several shear zones. Gneisses and supracrustal rocks of amphibolite facies are abundant along with granulite facies rocks. The radiometric dates obtained from SGT show the ages mostly vary between 3000 to 2000 Ma (Chakrabarti et al., 2006; Plavsa et al., 2012). Dharwar craton (3200 to 3400 Ma) is one of the oldest craton in the Indian shield (Valdiya, 2010). According to Rogers (1986), the Dharwar craton is further divided in two tectonic blocks - western Dharwar craton (WDC) and eastern Dharwar craton (EDC), (Fig 2.2) and the entire Dharwar craton is considered to have

formed by the accretion of WDC and EDC at 2750-2510 Ma. The zone of accretion is marked by a shear zone, which is variously referred to as the Chitradurga shear zone (CSZ) (e.g. Chadwick et al., 1999; 2000; 2003; Meert et al., 2010).

According to Ramakrishnan and Vaidyanadhan (2010), the Closepet granite that lies to the east of the CSZ is the western margin of EDC. The contact between WDC and EDC is not sharp and there is a transition zone between Chitradurga shear zone and Closepet granite. The EDC is considered to have formed with island arc accretion to an older (>3500 Ma) solid WDC through transpression (Balakrishnan et al., 1999; Manikyamba et al., 2005). The WDC occupies major portions of Peninsular Gneisses and it exhibits various Younger granites (~2600 Ma) are mainly exposed in the Chitradurga, Hosadurga, and Jampalnaikankote (J.N. Kote) region as isolated plutons. The WDC is significantly different from EDC (shown in Table 2.1) in terms of nature and abundance of greenstones as well as the age of surrounding basement rocks (Rollinson et al., 1981). The Archaean TTG is found throughout the WDC and dated to be 3300 - 3400 Ma (Pitchamuthu and Srinivasan, 1984; Bhaskar Rao et al., 1991; Naha et al., 1991). Three generations of volcano sedimentary greenstone sequences are recorded in the WDC: the 3100 - 3300 Ma Sargur Group, the 2600 - 2900 Ma Dharwar Supergroup, the 2500 - 2600 Ma calc-alkaline to high potassic granitoids (Radhakrishna and Vaidyanadhan, 1997). The regional metamorphic grade of WDC increases from greenschist facies in north to granulite facies in south. In the following table, only the brief aspects of the regional stratigraphy are presented.

Chitradurga- Gadag Superbelt:

The NNW-SSE trending Chitradurga-Gadag linear superbelt covers an area of 6000 km^2. Lithologically, the schist belt represents the thick volcano-sedimentary suite. The dominant rock types of the Chitradurga Schist belt include metabasalt and metagreywacke-argillite sequences interspersed with bands of quartzite, polymict conglomerate and BIF (Sengupta and

Age	Western Dharwar Craton (WDC)	Eastern Dharwar Craton (EDC)
2500-2600 Ma	Younger granite (Chitradurga, Arsikere) Charnockite	Younger granite/ Gneiss (closepet and equivalents) Charnockite
2600-2800 Ma	Chitradurga Group / Babadudan Group — Dharwar Supergroup — Kolar Group / Yashwantanagar Formation	
	---------- unconformity ----------	
~3000 Ma	Peninsular Gneiss	Enclaves older gneiss
3100-3300 Ma	Sargur Group	(?) Warangal Group (?) Salem Group
3300-3400 Ma	Gorur Gneiss	Putative Basement

Table 2.2 Simplified stratigraphy of western Dharwar craton (WDC) and eastern Dharwar craton (EDC) (after Swami Nath and Ramakrishnan, 1981).

<table>
<tr><td colspan="5">Proterozoic mafic dykes
Charnokites (2500 - 2600 Ma)
Younger granites (2600 Ma)</td></tr>
<tr><td rowspan="3">Dharwar Supergroup (2800 - 2600 Ma)</td><td rowspan="2">Chitradurga Group</td><td>Ranibennur Subgroup</td><td colspan="3">Greywackes with BIF, polymict conglomerate, volcanic (Maradihalli, Bellara, Medur)</td></tr>
<tr><td>Vanivilas Subgroup</td><td>Polymict conglomerates, cross-bedded quartzite, pelites, stromatolitic carbonates, biogenic cherts, BIF and Mn formation</td><td>Ingaldhal Volcanics</td><td>Tholeiitic basal-rhyolite suit (Tekalvatti, Jagar)</td></tr>
<tr><td colspan="2">Bababudan Group</td><td colspan="3">BIF and Carboneceous phyllites
Basalt-dacite suit (Locally pillowed) with minor ultramafics
Alternatnations of amygdular basalt, cross-bedded quartzites, pelites, minor BIF
Basal Quartz pebble conglomerates</td></tr>
<tr><td colspan="5">----------Fundamental Unconformity----------</td></tr>
<tr><td colspan="5">Peninsular Gneiss (ca. 3000 Ma)</td></tr>
<tr><td colspan="2">Sargur Group (>3000Ma)</td><td colspan="3">Ultramafic-mafic intrusive complexes (Holenatasipur, Nuggihalli)
Surpentinised komatiites, komatiitic and tholeiitic amphibolites, cherts, BIF
Garnet-biotite schist (with kyanite, sillimanite and staurolite)
Local marbles and calc silicates
Fuchsite quartzite with chromite and barites layer</td></tr>
<tr><td colspan="5">(?) Gorur Gneiss (3300 Ma)</td></tr>
</table>

Table 2.3 Regional stratigraphy of western Dharwar craton (after Swami Nath and Ramakrishnan, 1981; Ramakrishnan, 1994; Chakrabarti et al., 2006; Ramakrishnan and Vaidyanadhan, 2010)

Roy, 2012). Regionally, this belt is surrounded by older Peninsular Gneisses and younger granitoids (Ramakrishnan and Vaidyanadhan, 2010). In the western and eastern margin of the Chitradurga schist belt two granite bodies are exposed in the vicinity of Chitradurga town, known as Chitradurga granite and J.N. Kote granite respectively (Fig 2.3). In the present study, horizontal surface outcrops from the NW and SE ends of the pluton of Chitradurga Granite are taken for topological analysis. Available radiometric ages on the Chitradurga granite suggest that the crystallization age of the granite is 2614 ± 10 Ma (SIMS U–Pb dating zircons; Jayananda et al., 2006), which also similar to the age of whole rock Pb-Pb isochrones yielding an age of 2605 ± 18 Ma (Taylor et al., 1984).

A series of variably plunging synclines and anticlines with steep NNW-SSE trending axial planes are common in the Chitrdurga schist belt. The major structure is Chitradurga anticline, upright fold with undulating axial plane and near vertical plunge (Ramakrishnan and Vaidyanadhan, 2010). The anticline is flanked on either side by synclines and interpreted as a second generation folding. A major sinistral shear zone marks the eastern boundary of the schist belt. The structural investigations of the adjacent metasedimentary rocks of the region reveal that the area has undergone three phases of deformation: D1, D2 and D3 (Chadwick et al., 1989; Jayananda et al., 2006). Regionally D1/D2 are coaxial with NW-SE striking axial plane. D1 folds are reported as tight, isoclinal fold whereas D2 folds are open to tight and upright. D3 folds (regional open; NE-SW striking vertical axial plane) superimpose the earlier structures, forming culmination and depression in the region (Chakrabarti et al., 2006). According to

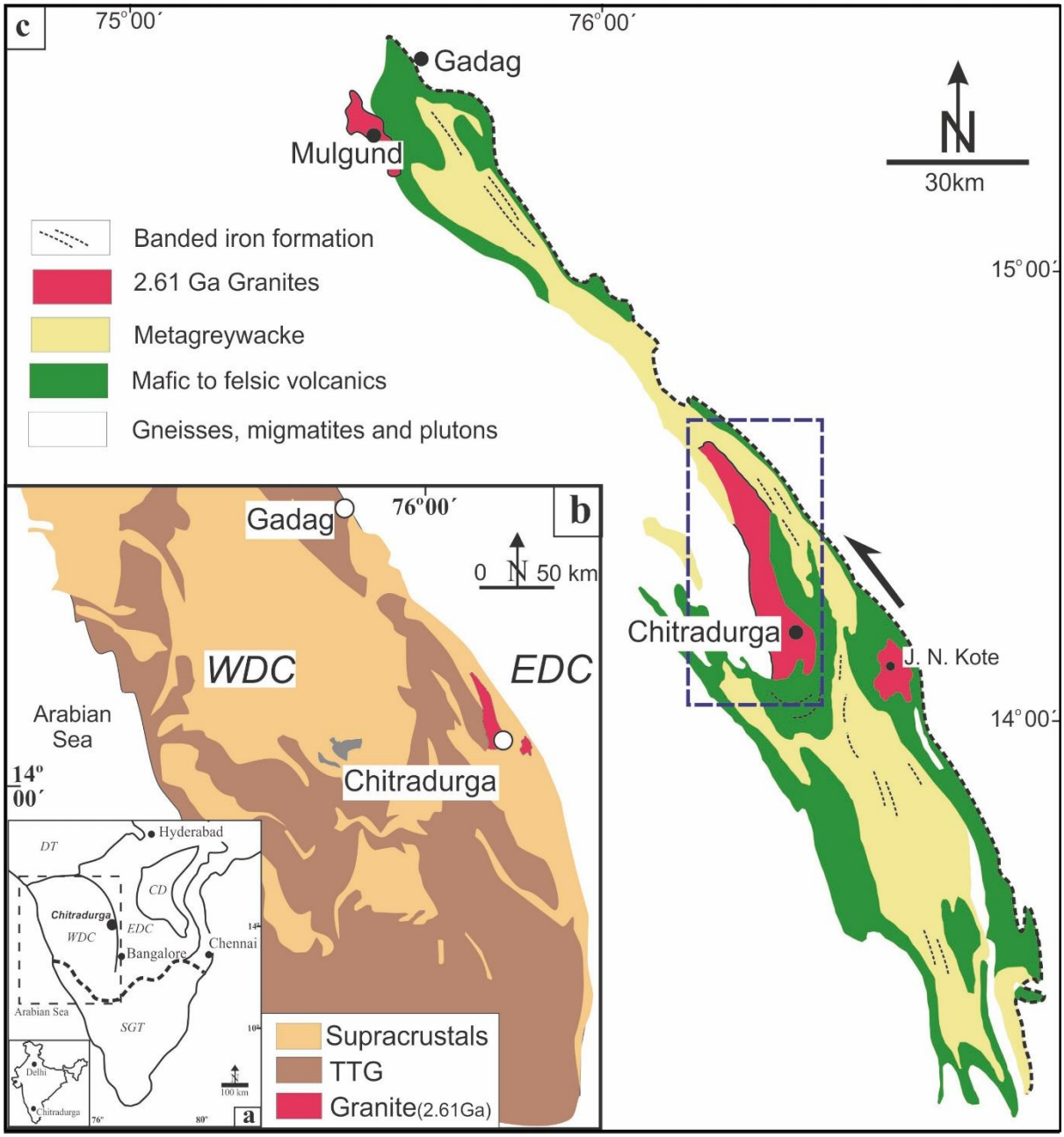

Fig 2.3: Map showing regional geological features of the Chitradurga Schist Belt. The dashed box indicates the study area, shown in Fig 2.4. Map modified after Mondal (2018).

Sengupta and Roy (2012), NE-SW directed shortening was responsible for the development of NW-SE oriented structural elements (D1/D2 deformation) in the Chitradurga schist belt, whereas D3 deformation was on account of NW-SE shortening. Thus, the above studies

indicate that the structural evolution of the Chitradurga schist belt is controlled by early NE-SW compression followed by late NW - SE compression.

2.3 Geology of the study area

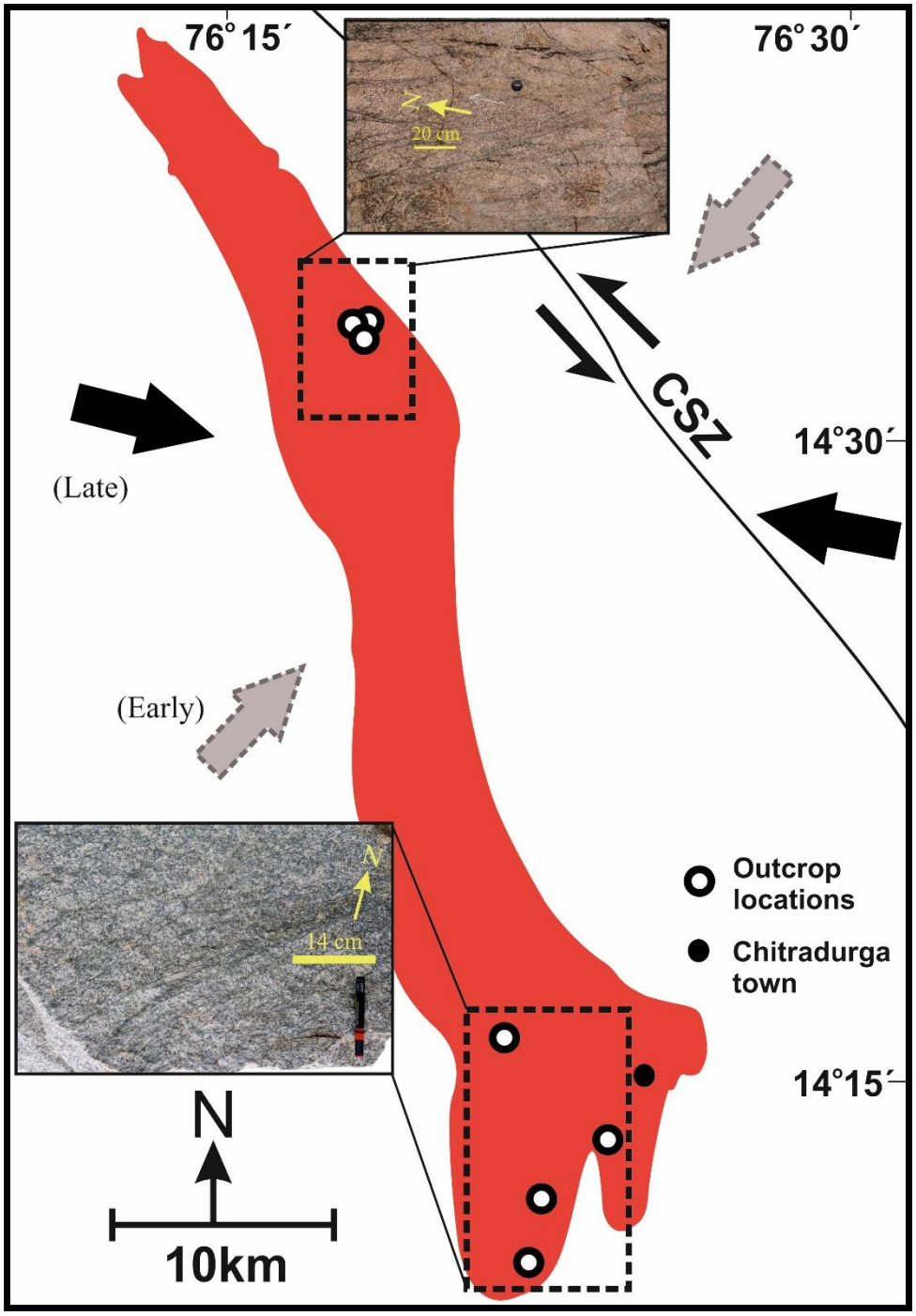

Fig 2.4: Map of Chitradurga Granite (modified after Mondal and Acharyya; 2018), showing the outcrop locations for the present study, some sample fractured outcrops, and the established paleostress directions (black and grey arrows) (after Mondal; 2018)

The Chitradurga granite is massive and in most outcrops lack a well-developed foliation; shows micro-granitoid enclaves at few places, which suggest that the granite has formed by reworking of early crustal rocks (Jayananda et al., 2006). Geophysical (gravity) investigations indicate that the disposition of Chitradurga granite in NW-SE direction and depth persistence to be 6 km (Rama Rao et al., 2015). The granite is coarse grained, equigranular and broadly homogeneous in composition. The composition varies from granite to granodiorite with biotite as major mafic mineral. At some places the granite shows the occurrence of solid state fabric in the form of minor shear zones. Although, the granite is devoid of mesoscopic fabric, at places, it shows well developed foliation, particularly in the northern region and the granite margin. The foliation in granite, defined by the planar shape preferred orientation of quartz and feldspar grains, strikes ~NW-SE and dips steeply to the NE (mean strike/dip is 316°/63°). This orientation is parallel to the foliation orientation recorded from the adjacent metasedimentary rocks as well as regional trend of the CSZ. The sub-horizontal stretching lineations on the foliation plane are also observed at some places. The stretching lineations show shallow plunge either to the NW or the SE (Mondal, 2018). Bhatt et al. (2017) argues that age of the D1/D2 deformation phase is $\geq$ 2549 Ma, while D3 is $\leq$ 2537 Ma, from the study of Koppal granitoid, another syn-tectonic plutonic body whose emplacement is associated with D1/D2 deformation.

In the next chapter, the methodology which has been followed in this study has been described in detail, along with the components of topology as well as the FracPaQ toolbox.

CHAPTER 3

Methodology

3.1 Introduction

In the present work, the method of analysis of fractures from 2D outcrops as put forward by Sanderson and Nixon (2015, 2018) are used. They introduced the concept of topology as a system of properties that are unchanged by continuous transformation, such as strain of the space in which the studied objects (here, fractures) are embedded. Such a transformation, changes the geometrical properties, viz. length, orientation, but not the topology. So we can understand that in order to be scale and continuous transformation invariant, topology must involve dimensionless parameters. Such an approach can be made with the method of node and branch topology, which in two dimensions, recognizes a fracture network as a system of branches and nodes, which would be the basis to provide important additional parameters to

characterize the network. Hence topology allows us not only to characterize the fractures, but also estimate some properties of the fracture network.

3.2 Network topology

Topology has been a tool for characterizing and describing complex network structures for a wide range of subjects. In general, topology describes the relationships between geometrical elements of a network (Jing and Stephansson, 1997). Unlike geometrical attributes such as length, thickness, and spacing that are measured by defined dimensional units, topological attributes are dimensionless (Jing and Stephansson, 1997). Topology is important in the assessment of the connectivity of a fracture network, which is essential to understand fluid flow and transport properties. So there has been some recent work regarding application of topological analysis to fracture network models in order to evaluate the connectivity of fracture networks (Jing and Stephansson, 1997; Manzocchi, 2002). These studies use a variety of parameters calculated from different topological components to quantitatively assess connectivity, such as number of intersections per line (Manzocchi, 2002), the density of intersections and the efficiency of connectivity, which evaluates the ability of a network to connect two different points to one another.

Topological components within fracture networks can be evaluated in two and three dimensions. In three dimensions, a network consists of fracture planes, which terminate at tip lines or produce intersection lines, and divide the host rock mass into blocks. On the other hand, in two dimensions, a network consists of fracture traces, which terminate at points

(fracture tips) or intersect and abut one another, diving the surface area into un-fractured compartments. In our present study, we consider the topology of 2D fracture networks,

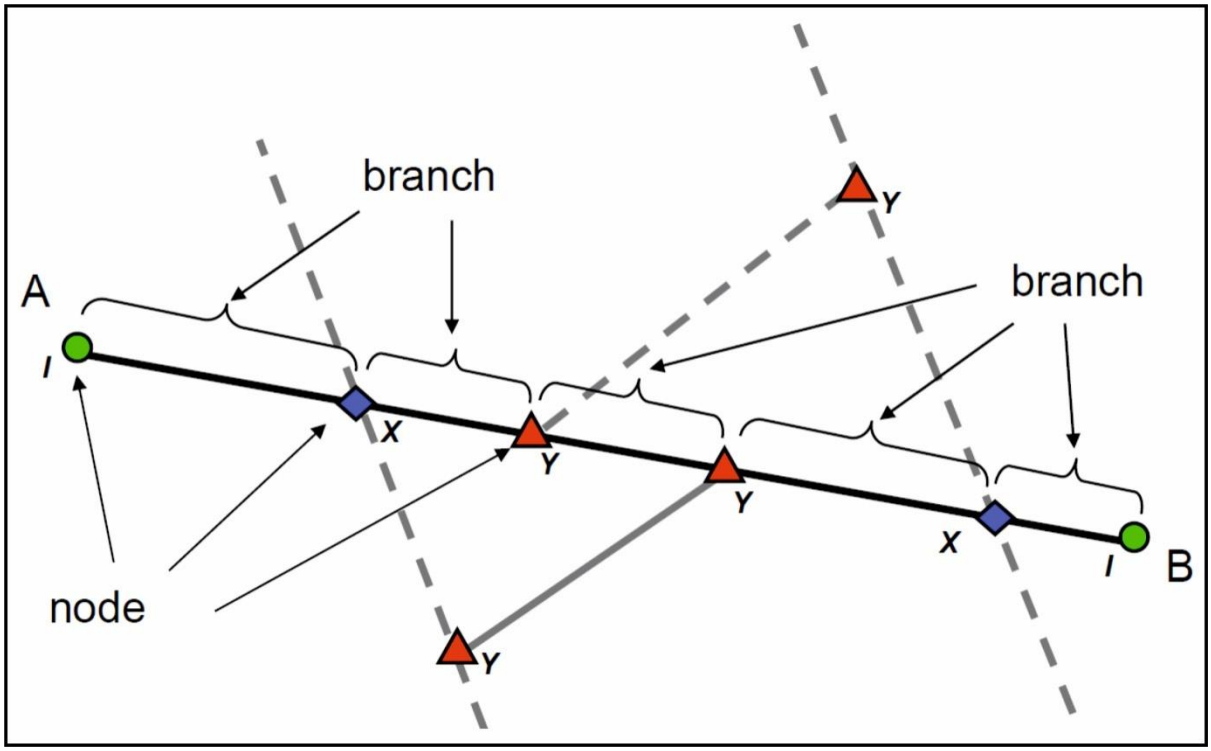

Fig 3.1 Fracture trace (A-B), with associated intersecting fractures (dashed), showing arrangement of nodes and branches: I-nodes (circles); Y-nodes (triangles); X-nodes (diamonds). After Sanderson and Nixon (2015)

concentrating on the topological components that describe the fractures within the network (viz. trace length, tips, abutments, intersections). As mentioned before, we shall primarily concentrate on the node-and-branch approach, where we consider the topology of a 2-D fracture network to consist of lines, nodes and branches, where each line consists of one or more branches with a node at each end. Following Manzocchi (2002), nodes can be divided into three types, isolated fracture tips (I-nodes); crossing fractures (X-nodes) (Fig 3.1); and abutments or splays (Y-nodes). In the case of a random array of lines, each line will consist

of two I-nodes, with additional intersections represented by X-nodes. For many 'natural' fracture networks, however, fractures terminate against (or abut) pre-existing fractures, producing many Y-nodes. I-nodes do not connect any branches whereas X-nodes and Y-

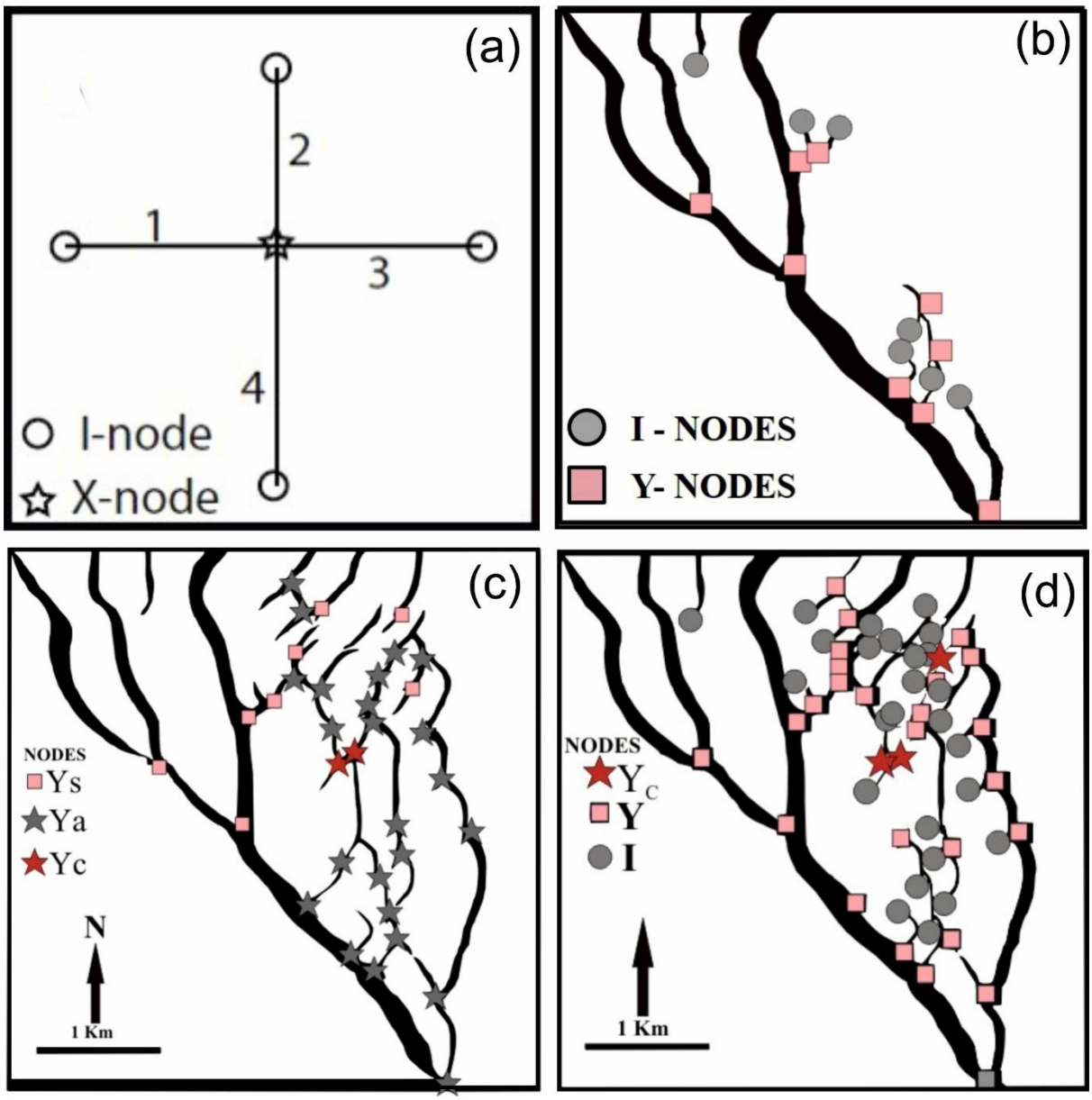

Fig 3.2 The types of nodes used in node-and-branch approach of topology, as applied in natural fault networks of Phitsanulok Basin, Thailand. In addition to I, Y and X nodes, three more node types are shown in (c) and (d); those being Ys, Ya and Yc. Yc node is a point where one fault offsets another. Geologically similar to an X-node except there is offset so that topologically the node is Y-type. Ys and Ya are subdivisions of Y-node for splaying and abutting geometries respectively.Modified after Morley and Nixon (2016).

nodes connect 4 and 3 branches, respectively. The branches themselves have a node at each end and can be described by these two nodes such as I-I, I-X, I-Y, X-Y etc. As nodes can be divided into connecting (C) i.e. X or Y-nodes and isolated (I) nodes, we can further classify the branches into three main topological groups: I-I branches, I-C branches, C-C branches.

3.3 Dimensionless parameters derived from node counts

The proportion of I-, Y- and X-nodes can be used to characterize a fracture network (Manzocchi, 2002), and these proportions may be plotted on a triangular plot. Such a classification is topological rather than geometrical as it is unchanged by any continuous transformation of the network. Since I- and Y-nodes represent the tip of one line, the number of lines (N_L) is given by:

$$N_L = \tfrac{1}{2} (N_I + N_Y) \quad (1)$$

Each branch will have two nodes, with an I-node contributing to one branch, a Y-node to 3 branches and an X-node to 4 branches.

Hence the number of branches (N_B) is:

$$N_B = \tfrac{1}{2}(N_I + 3N_Y + 4N_X) \quad (2)$$

Thus, the ratio of number of branches to lines is:

$$N_B / N_L = (N_I + 3N_Y + 4N_X)/(N_I + N_Y)$$

$$= (P_I + 3P_Y + 4P_X)/(P_I + P_Y) , \quad (3)$$

where ,P_I, P_Y and P_X represent the proportion of each type of node. Since $P_I + P_Y + P_X = 1$, or

$P_X = 1 - P_I - P_Y$, equation 3 can be written as:

$$N_B / N_L = (4 - 3P_I - P_Y) / (P_I + P_Y) \quad (4)$$

Equations (1) to (4) allow us to determine the number of lines or branches by simply counting the number of nodes. In addition, these equations also allow us to convert the number of lines to the equivalent number of branches. Since the definition of a complete line or branch requires 2 nodes, it is implicit in equation (1) to (4) that lines and branches that extend beyond the sampled area are counted as ½ and that those cutting through the area of sampling will be omitted from the analysis of that area. In this way lines are only counted a total of once in non-overlapping sample areas.

The connectivity of a network can be described in terms of the average connection per line C_L. As each connecting node provides a connection on two lines then,

$$C_L = 2N_C / N_L = 2(N_Y + N_X) / N_L \quad (5)$$

Connectivity can also be represented by the number of connections per branch C_B. As each Y-node connects 3 branches and each X-node connects 4 branches, so

$$C_B = (3N_Y + 4N_X) / N_B \quad (6)$$

The number of connections per line C_L has been widely used as a measure of connectivity (Manzocchi, 2002), however, C_L, is not independent of topology, which would be evident in

following section. C_B is a dimensionless number in the range of 0-2 that is a useful measure of connectivity.

3.4 Ternary diagrams

The proportions of each topological component (nodes and branches) provide information about the organization of fractures within a fracture network. Manzocchi (2002) had plotted the proportions of I, Y and X-nodes in ternary diagram (Fig 3.3). Where the statistics of the particular studied network plots inside the diagram represents the networks connectivity, with networks becoming more connected the further away they plot from the I-node corner (Manzocchi, 2002). Nixon et al. (2012) also use the ternary diagram to show the connectivity

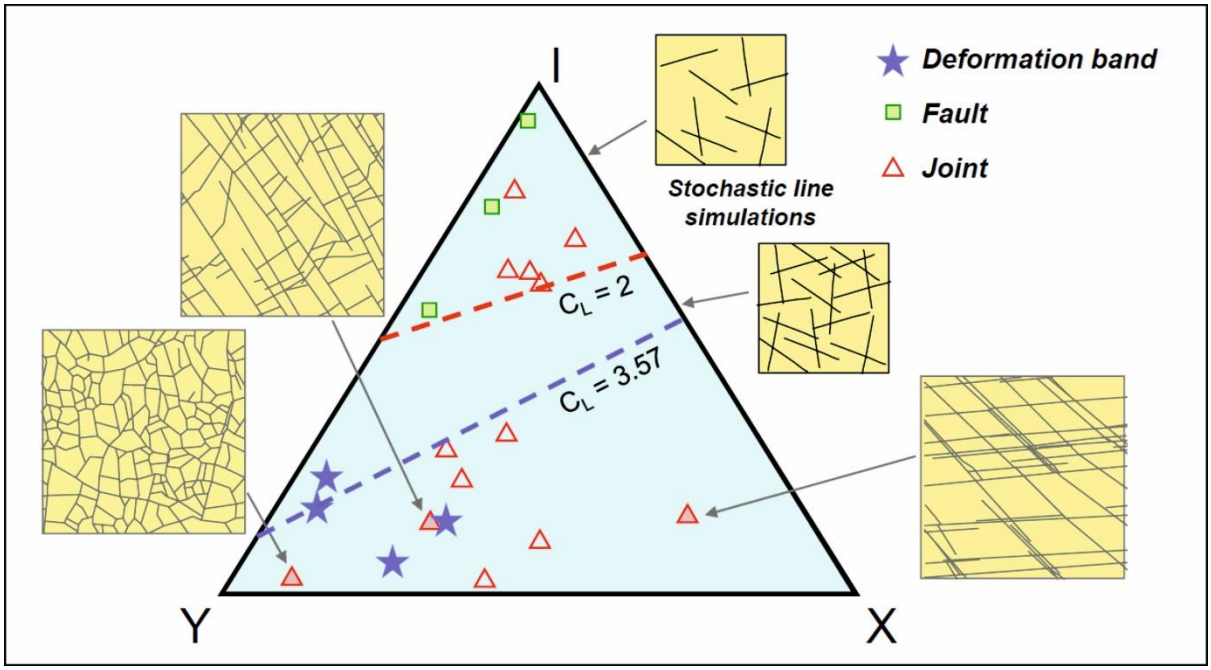

Fig. 3.3 Triangular plot of the proportion of node types for different networks (after Manzocchi (2002) and Sanderson and Nixon (2016)). Three natural fracture networks (from Sanderson and Zhang (1999)) and two random line simulations show how the fracture network topology is characterized. The dashed lines show specific numbers of intersections per line, with $C_L = 2$ representing a limit above which a spanning cluster is not possible and $C_L = 3.57$ the value widely reported from random line simulations.

of fault networks and, hence, this is used for the nodal analysis in this study as well.

The intimate dependence of connectivity value C_L on topology can be illustrated as networks with no isolated nodes plot along the X-Y axis and would be completely connected, yet have very different values of C_L. C_B on the other hand is not dependent on topology as equation 6 is not entirely topology dependent.

Node counting provides an unbiased estimate of frequency and can be used in conjunction with fracture intensity to estimate the characteristic length and dimensionless intensity of the fractures (see next section). The latter provides a measure of fracture development that is independent of scale and has many practical applications. The fracture intensity (number of fracture intersections per unit length, line length per unit area, surface area per unit volume) is the most fundamental measure of fracture abundance and has units of $[L]^{-1}$. Raw measurements can easily be corrected to provide an unbiased estimate and such estimates are equivalent for sampling in different dimensions.

3.5 Measuring fracture abundance and size

Fractures can be sampled in one, two or three dimensions. In this study, we focus on 2-D sampling of fracture data. Information on the fractures may simply be their number (or frequency), trace length or surface area. Dershowitz and Einstein (1988), and Dershowitz and Herda (1992) defined a number of measures of fracture abundance by P_{xy}, where x denotes the dimension of the sampling region and y the dimension of the feature being measured.

Frequency is used for any sample of the number of fractures (N_L), and can be normalized by the line length (L), sample area (A) or volume (V) to define:

Linear frequency: $F_L = P_{10} = N_L / L$ with dimension $[L^{-1}]$

Areal frequency: $F_A = P_{20} = N_L / A$ with dimension $[L^{-2}]$

Volumetric frequency: $F_V = P_{30} = N_L / V$ with dimension $[L^{-3}]$

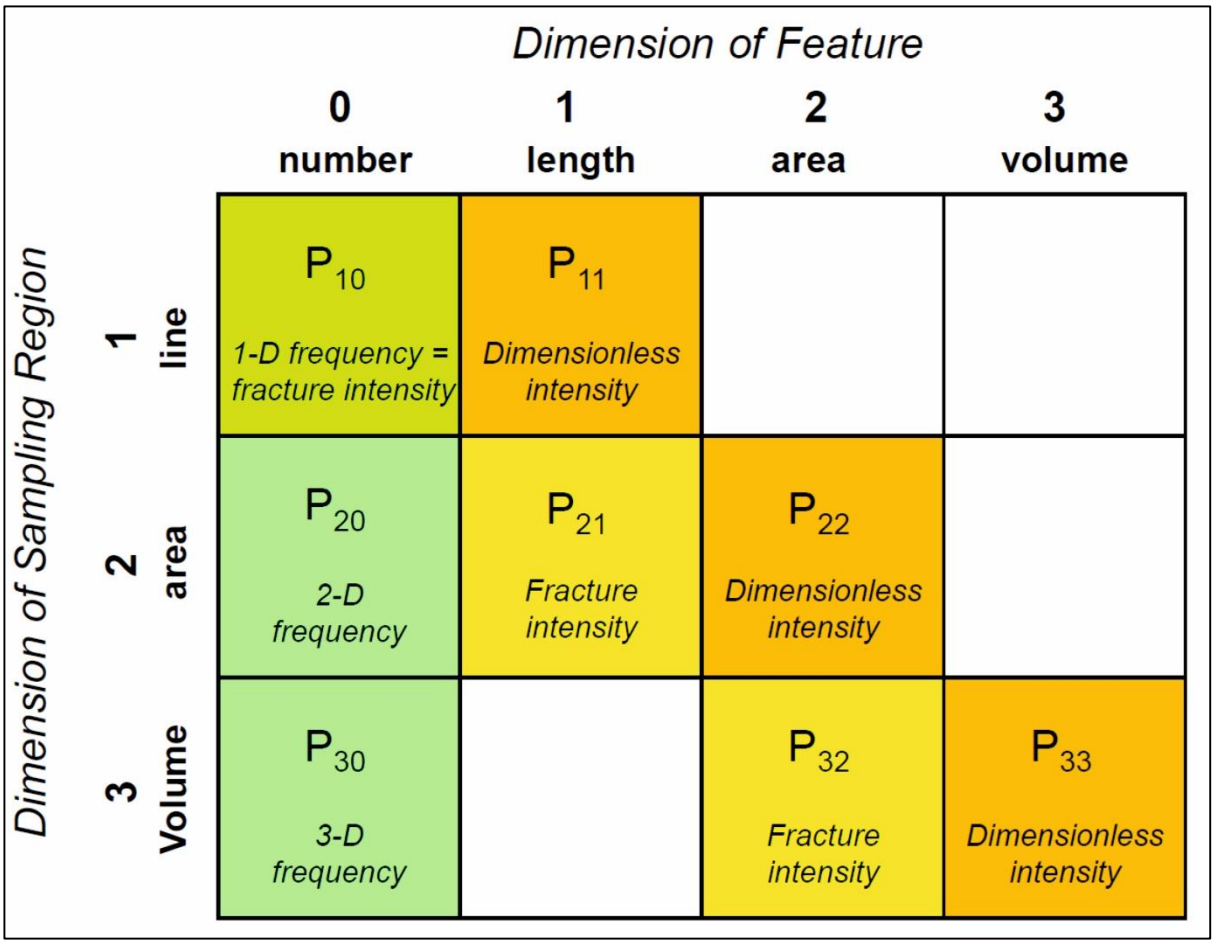

Table 3.1 The system of measurement by the P_{XY} system (after Dershowitz and Einstein, 1988). The columns show the dimensions of the features measured; the rows represent the dimension of the sampling region. The dimensionless intensity is obtained by multiplying the fracture intensity in each row by the characteristic fracture length. Figure after Sanderson and Nixon (2015)

The term fracture intensity is used to express the total trace length per unit area, as originally suggested by Dershowitz and Einstein (1988). Here fracture intensity has dimensions [L^{-1}], and the concept is extended to 1- and 3-dimensions for measures with the same dimensions. This term is often referred to as fracture density in previous literature (e.g. Nixon et al., 2012).

The term dimensionless intensity is reserved for measures that are dimensionless [L^0]. So instead of the term density, which may sound confusing, the term intensity is used throughout this work. Thus in 2-D areas, there are 3 possible measures of fracture abundance:

Aerial frequency: $P_{20} = N_L / A$ with dimension [L^{-2}]

Fracture intensity: $P_{21} = \Sigma L / A$ with dimension [L^{-1}]

Dimensionless intensity: $P_{22} = N_L.L_C^2 / A$ with dimension [L^0],

where, L_C is the characteristic length, and is most simply defined as the arithmetic mean of the line lengths, hence:

$$L_C = \Sigma L / N_L$$

In practice, the simplest way to determine P_{22} and L_C is to determine the aerial frequency (P_{20}) and fracture intensity (P_{21}) and from the above equations:

$$P_{22} = (P_{21})^2 / P_{20} \quad \text{and}$$

$$L_C = P_{22} / P_{21} = P_{21} / P_{20}$$

These were the broad concepts used for the present analysis.

3.6 Digital analysis using FracPaQ

FracPaQ is a fracture analysis toolbox based on MATLAB platform (Healy et al. 2017), designed to quantify fracture patterns in 2 dimensions from digital data. The input can either

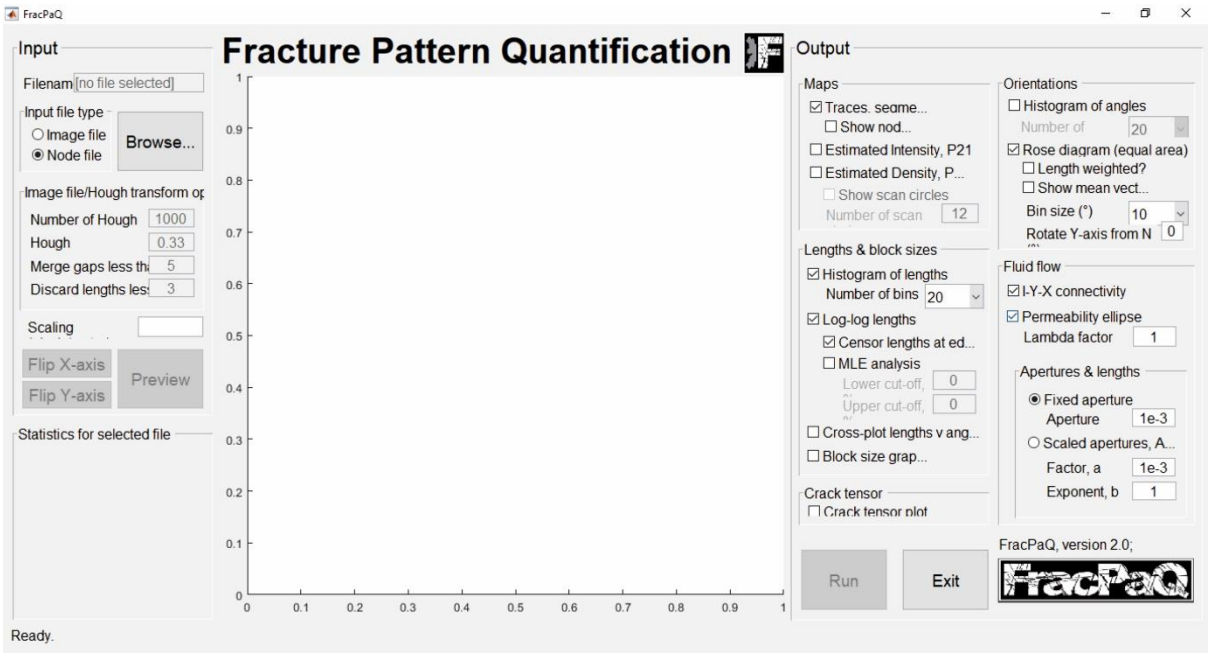

Fig 3.4 Screenshot of the graphical user interface (GUI) of the FracPaQ version 2.0. This is the only input window. Each output (map, graph etc.) is directed to a separate MATLAB™ figure window and saved to a separate graphics file.

be a binary image file of fracture traces, like a .jpg/.jpeg or .tif/.tiff image, or an ASCII tab-delimited text file of (x,y) coordinates that mark the nodes of each fracture trace. It is designed to generate quantitative fracture pattern data with user control over the output. The outputs from the toolbox include quantitative estimates of the attributes of individual

fractures (ex. lengths and orientations) and for the attributes of the whole pattern (ex. connectivity and permeability).

The mechanism which was used to prepare sample images for this analysis is a two step-process:

a) Importing the digital photograph of the outcrop into CorelDraw(R) and then manually tracing the fractures with a pen or polyline tool; thus generating polyline elements onto a new layer.
b) Exporting the layer with the fracture traces (without the underlying photograph) as a scalable vector graphics file (.svg), so that traces are saved as ‘line’ and ‘polyline’ tags.

The present version of FracPaQ assumes that the traced fractures lie on a statistically flat surface, so that the effects of topography on the appearance of fracture traces does not require correction. The quantification of lengths and orientations is then reduced to simple operations in coordinate geometry. In the algorithm of FracPaQ, a fracture trace is a continuous line composed of one or more straight fracture segments. Fractures at any scale are believed to have formed from the interaction and coalescence of smaller fractures. So for this reason, the graphs of length statistics are separated into plots for fracture trace lengths and fracture segment lengths.

The orientation distribution in a fracture pattern is important for unravelling the tectonic history of the rocks and in controls rock mass behaviour with respect to attributes such as permeability and strength. While plotting the rose diagram of the fractures, FracPaQ takes care of the issue of avoiding the inherent bias in a common linear form of the plot. To avoid this bias, the area of each sector is plotted proportional to the frequency of orientations; along with plotting angles of fracture segments and not fracture traces, as a straight line drawn between two end nodes of a trace will give an inaccurate average of the segment angles.

FracPaQ provides two measures of spatial density calculated from the input 2D fracture data: fracture intensity, labelled P_{21} by Dershowitz and Herda (1992), has units of m^{-1} and is defined as thetotal length of fracture in a given area (hence units of $m/m^2 = m^{-1}$), and fracture density, labelled P_{20} by Dershowitz and Herda (1992), has units of m^{-2} and is defined as the number of fractures per unit area. To generate the I-Y-X ternary plot, FracPaQ loops through the whole data structure of fracture traces and segments and finds the mutual intersections (using line-SegmentIntersect.m).The relative proportions of I, Y and X nodes are then calculated with respect to the total number of intersections found, and the connectivity triangle is plotted. FracPaQ also plots two ‘contour’ lines of connectivity, for C_L = 2.0 and 3.57 where C_L is the number of connections (intersections) per line (or trace), after Sanderson and Nixon (2015), as mentioned in section 3.3.

So this chapter presented an in-depth discussion about the process of topology used to interpret the fracture networks. The following chapter will deal with the observations made and the analytical results, obtained using the aforementioned principles.

CHAPTER 4

Application

4.1 Introduction

In the present chapter, the results of the methodology (articulated in Chapter 3) applied to study the Chitradurga Granite (CDG) is shown categorically, in the sequence of:

i. Fieldwork observations,

ii. Digital analysis and

iii. Statistical results.

Fieldwork observations include structural investigations of outcrops of CDG, presenting only the relevant aspects, as the major introduction has been given in Chapter 2, section 2.3. The

process of topological and digital analysis has been mentioned in Chapter 3; hence here only the results will be shown.

4.2 Field observations

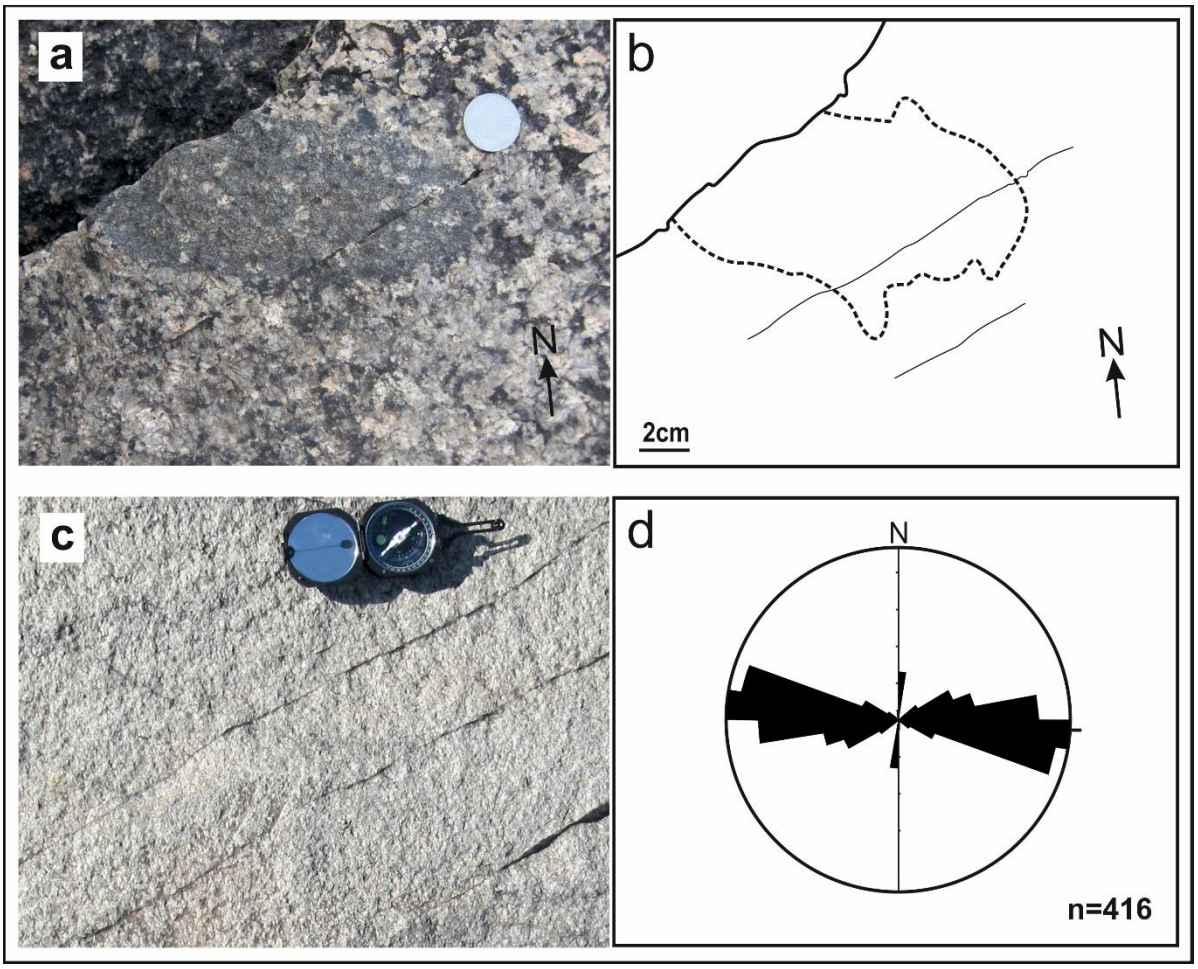

Fig 4.1 Field photographs after Mondal and Acharyya (2018) showing (a) a NE-SW trending fracture not restricted within the microgranitic enclave, established by Mondal and Acharyya (2018) to be thermal in origin, and (c) showing similar fractures seen in the host Chitradurga granite.

Due to the limited availability of horizontal, i.e. topographically flat outcrops of CDG, the entire study area of the pluton was divided into two sectors, Northern sector (CDGN) and Southern sector (CDGS). If we look at the regional map of the pluton, it might be noted that CDGN has a closer spatial association to the Chitradurga Shear Zone (CSZ), compared to

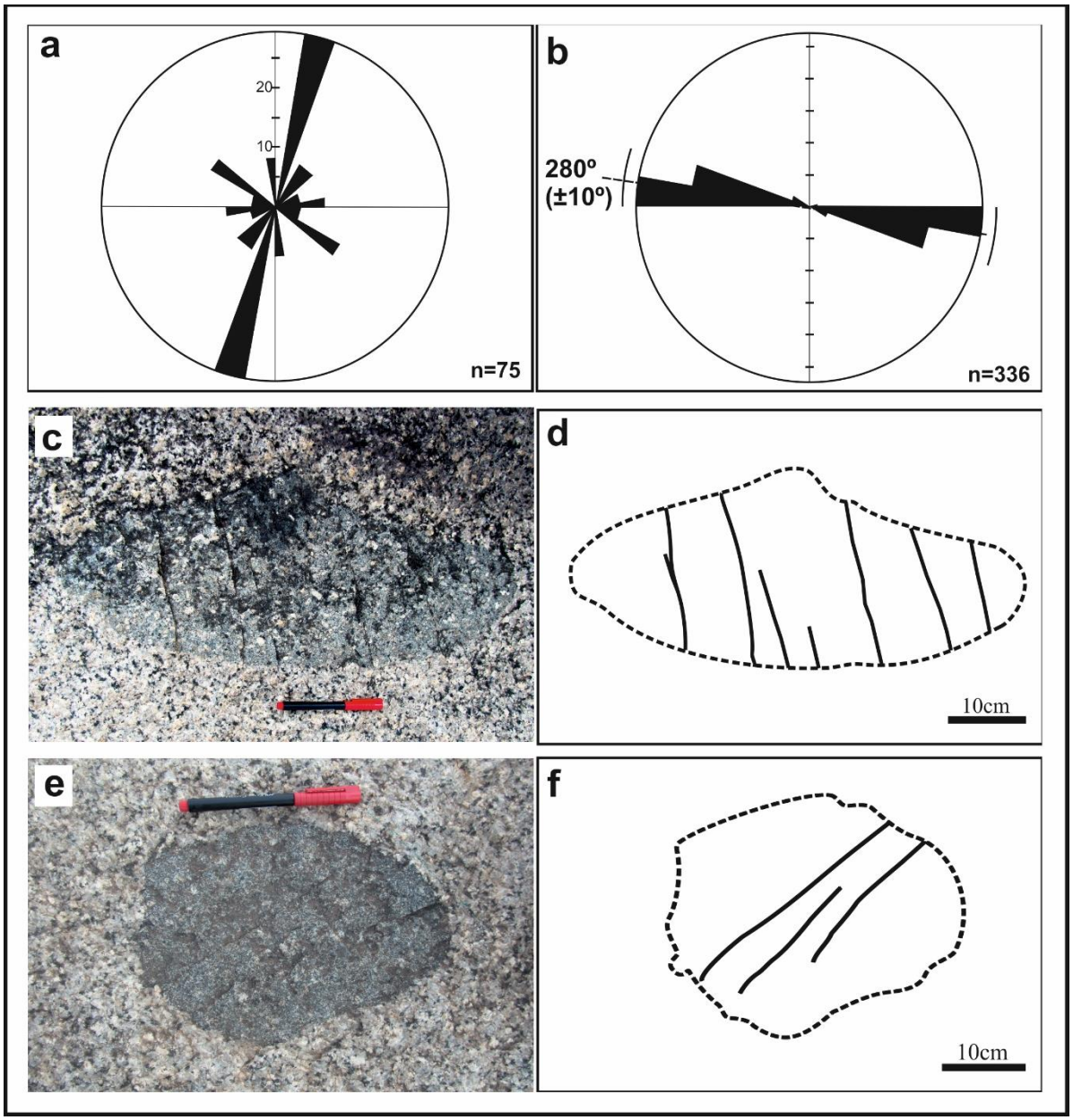

Fig 4.2 Field photographs after Mondal and Acharyya (2018) showing multiple, restricted and parallel fractures present within microgranitoid enclaves, established to be tectonic in origin.

CDGS. A total of five outcrops from the Northern and Southern sectors were analysed. The outcrops of CDGN showed fractures with a variety of orientations, but the majority showed a NNW-SSE trend, with variable dip angles. Moreover, the number of fractures present in an outcrop was appreciably high. In contrast, outcrops of CDGS showed a greater variety in

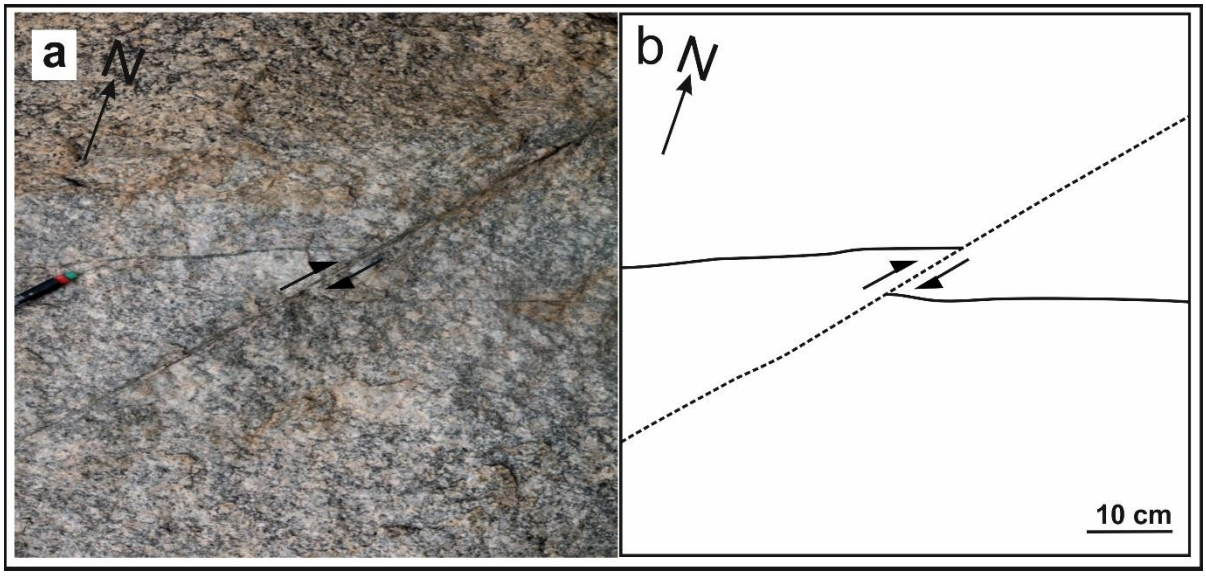

Fig 4.3: (a) Field photograph and (b) digital trace showing NE-SW thermal fracture displaced by post-emplacement dextral shearing, in the Chitradurga granite (after Mondal and Acharyya, 2018)

fracture trace orientations, with a sizeable majority showing NE-SW alignment. The dip angles were variable as in CDGN, between 40°and 70°.

The fracture apertures were not remarkably high, lacking any distinct vein formation. However, discolouration of the original appearance of the granite and presence of darker minerals in some fractures near Chitradurga Fort might indicate signatures of syn- or post-deformational fluid flow and alteration. According to Mondal and Acharyya (2018), the fractures of CDG have both tectonic and thermal origin; i.e. some fractures were initially produced due to thermal stress applied on the pluton during emplacement and cooling, which was followed by deformation events, leading to the formation of tectonic fractures. These two mechanisms of fracturing could not be distinguished in the field, where materials with contrasting rheology, viz. micro-granitoid enclaves, were not present.

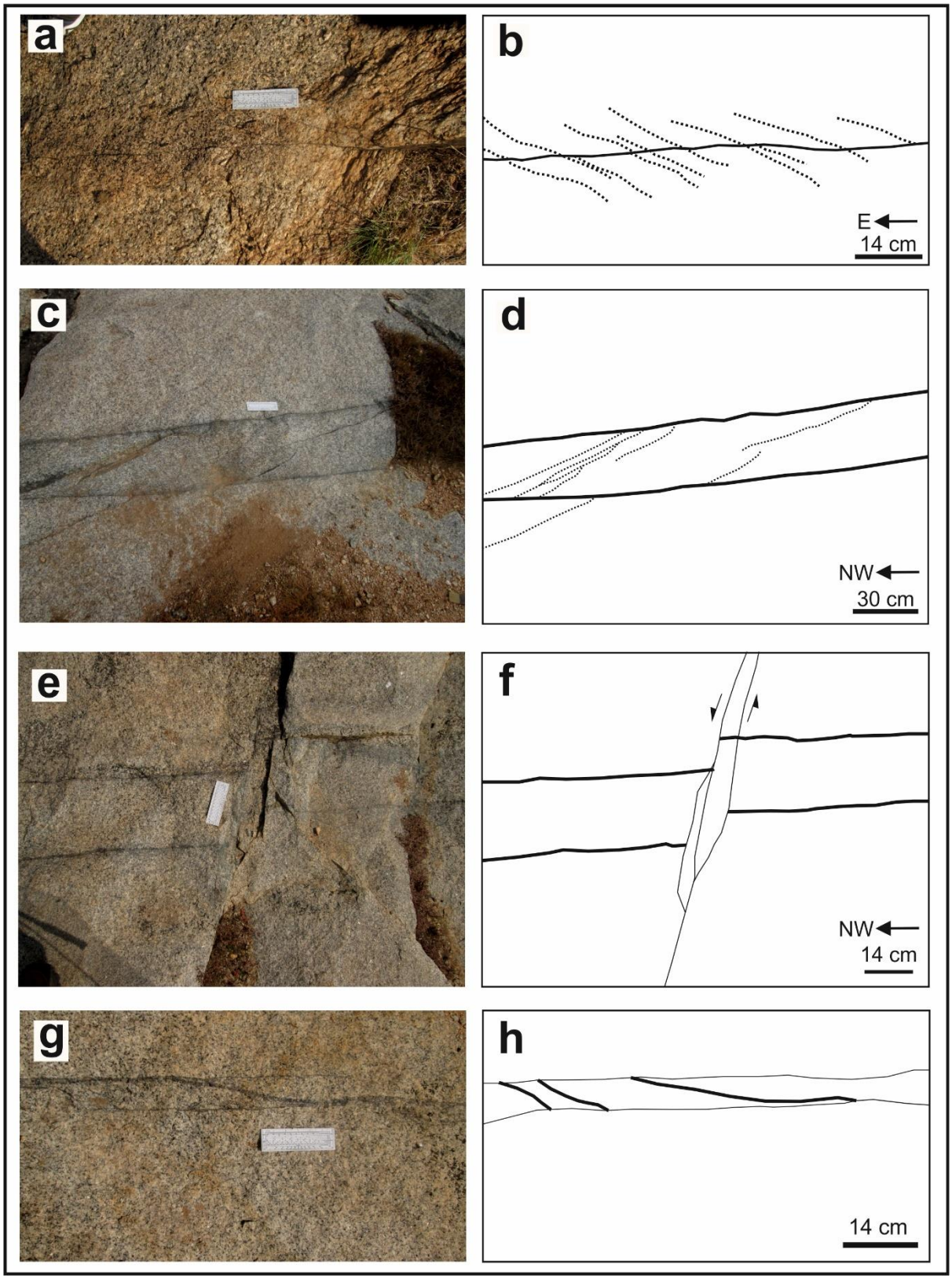

Fig 4.4 Field photographs and their trace sketches showing some characteristic features of the fractures in granite. (c) and (g) show bridging fractures, while (e) shows a sinistral shear offset of two fractures along another.

Though Mondal and Acharyya (2018) have explicitly concluded that steeply dipping fractures were attributed to a thermal origin, extensive fieldwork could not establish a threshold dip value which could be used to categorically distinguish these two mechanisms of fracturing.

4.3 Digital analysis and results:

This section will enlist the figures obtained by the analysis of digital photographs from Northern and Southern sectors, through FracPaQ, followed statistical results.

4.3.1 Northern sector

A representative horizontal outcrop near Petakonkuppe was chosen as the site for digital image acquisition. It was acquired through dividing the outcrop into grids and stitching the images of each individual grid was performed digitally, before feeding it as input in FracPaQ. The traced outcrop (Fig 4.9) is too chaotic to be interpreted manually using network topology. Fig 4.5 shows us

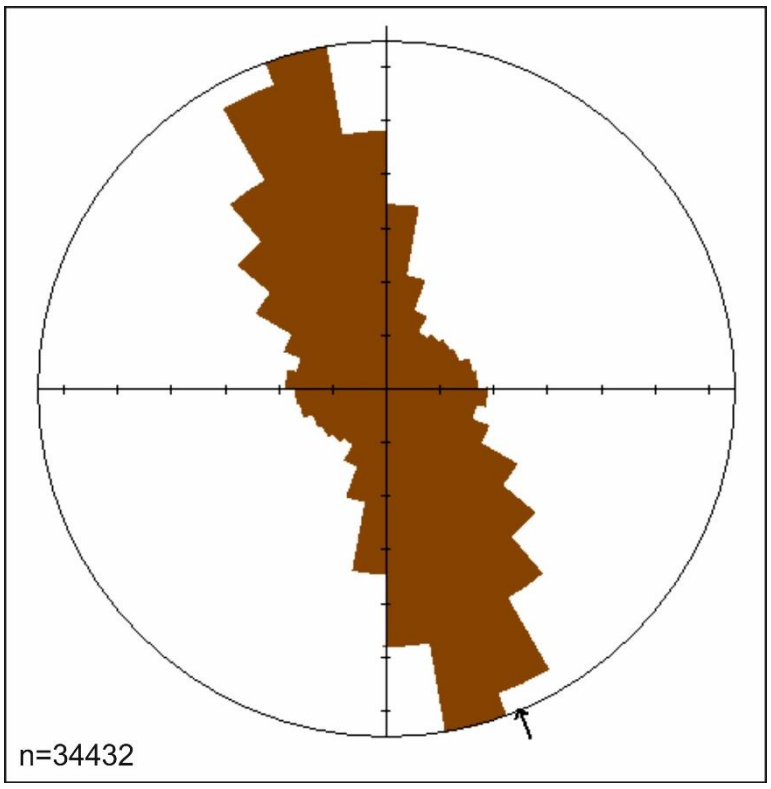

Fig 4.5: Rose diagram showing the major NW-SE orientation of fractures traced from the digital image of the Petakonkuppe outcrop. See Fig 4.9 for the traced outcrop.

the rose diagram of fracture trace orientation on the surface. Though a majority of the fractures shows a NW-SE orientation, there is a considerable spread in the fracture trends, ranging from E-W, to N-S, indicating overlapping phases of deformation. The number of fracture segments measured, 34432, is also significantly high for an area of ~ 16 square metres, indicating the intensity of brittle fracturing.

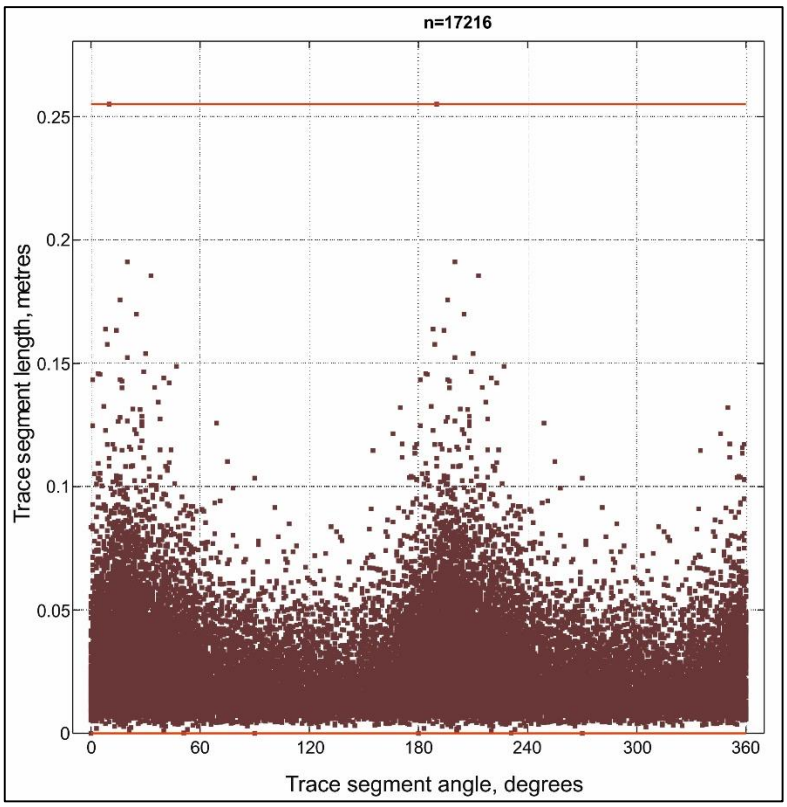

Fig 4.6: A plot of fracture trace segment length vs. their orientation, showing two definite major trends of the fracture traces. The red line demarcates maximum trace length.

Fig 4.6 shows us a pattern in the trend which is not visible in the outcrop trace. Here, we can clearly visualize two

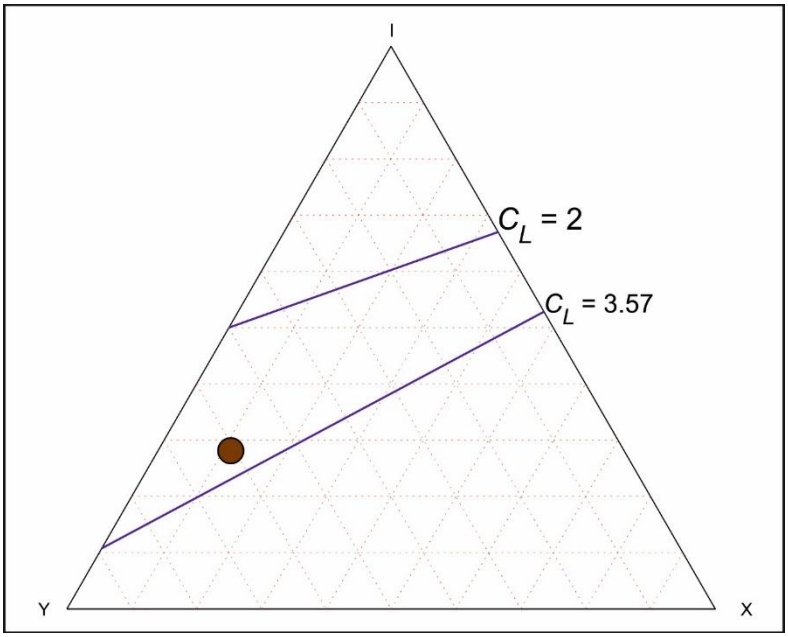

Fig 4.7: I-Y-X ternary diagram, obtained from FracPaQ, with the point showing the proportion of respective nodes in the Northern outcrop.

clustered orientation peaks among the fracture traces.

Fig 4.7 shows the I-Y-X ternary diagram (for more details see section 3.4), demarcating the position of the proportion of I, Y and X nodes as calculated from the Petakonkuppe outcrop. It can be seen that C_L shows a value between 2 and 3.57, near to the latter. The details will be dealt with in section 4.4.

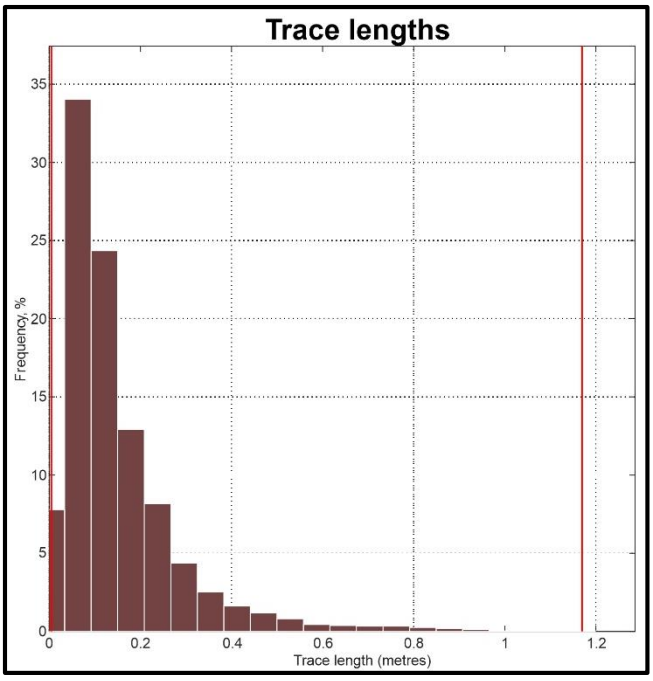

Fig 4.8: Histogram of fracture trace length of the Northern outcrop.

Fig 4.8 shows the histogram of fracture trace lengths, showing a very low size distribution of individual fractures, the maximum frequency being around 0.1m and the maximum trace length being less than 1m.

Fig 4.10 shows the fracture intensity map (P_{21}), showing significant areas with high values around 30-45 metre^{-1} (See section 3.5 for details). This supports the above observation that the area hosts a high intensity of brittle fractures.

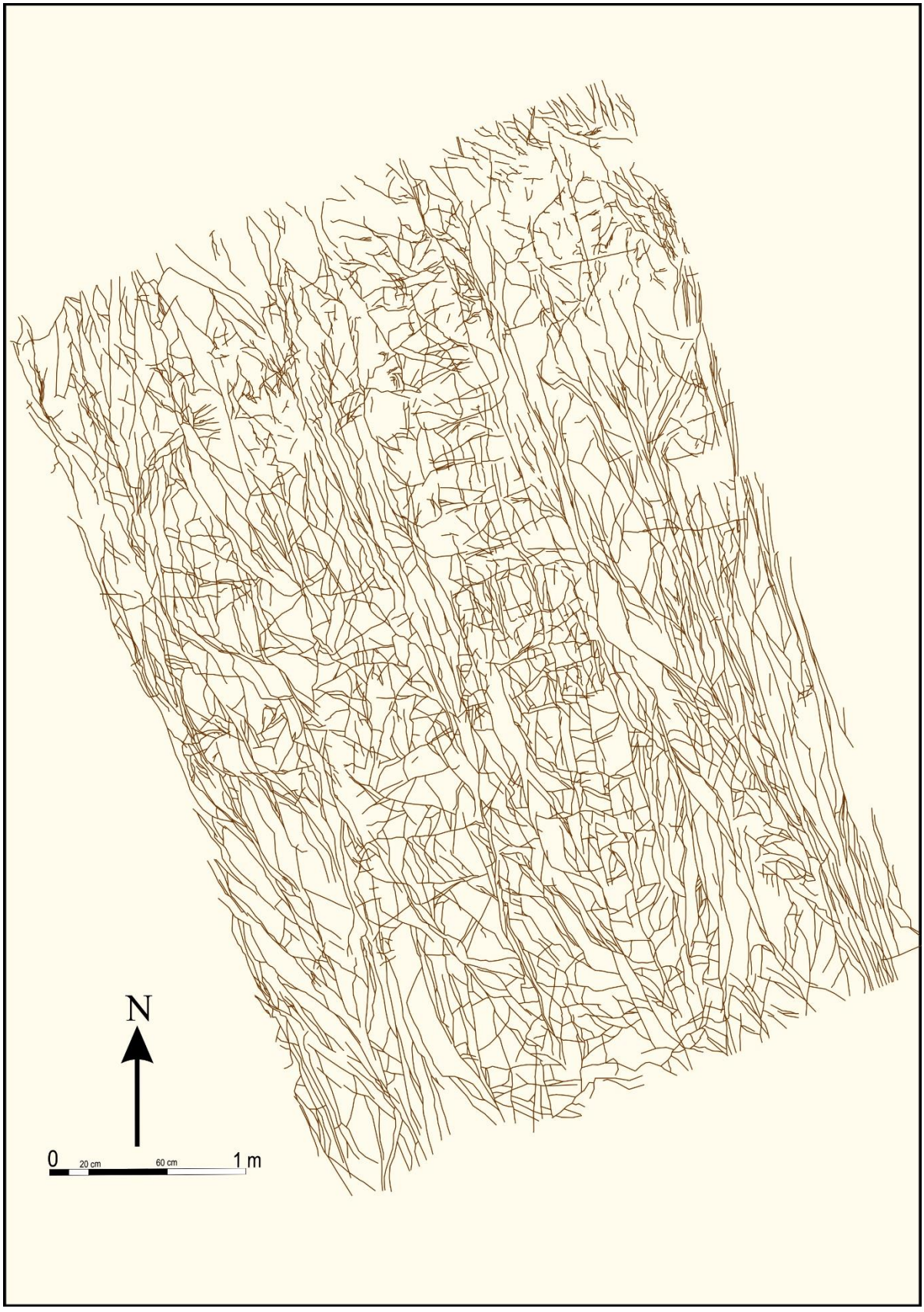

Fig 4.9: The digital fracture trace of the entire stitched outcrop of CDGN (Petakonkuppe), which was used as the input file for FracPaQ analysis, in an 8-bit binary image format.

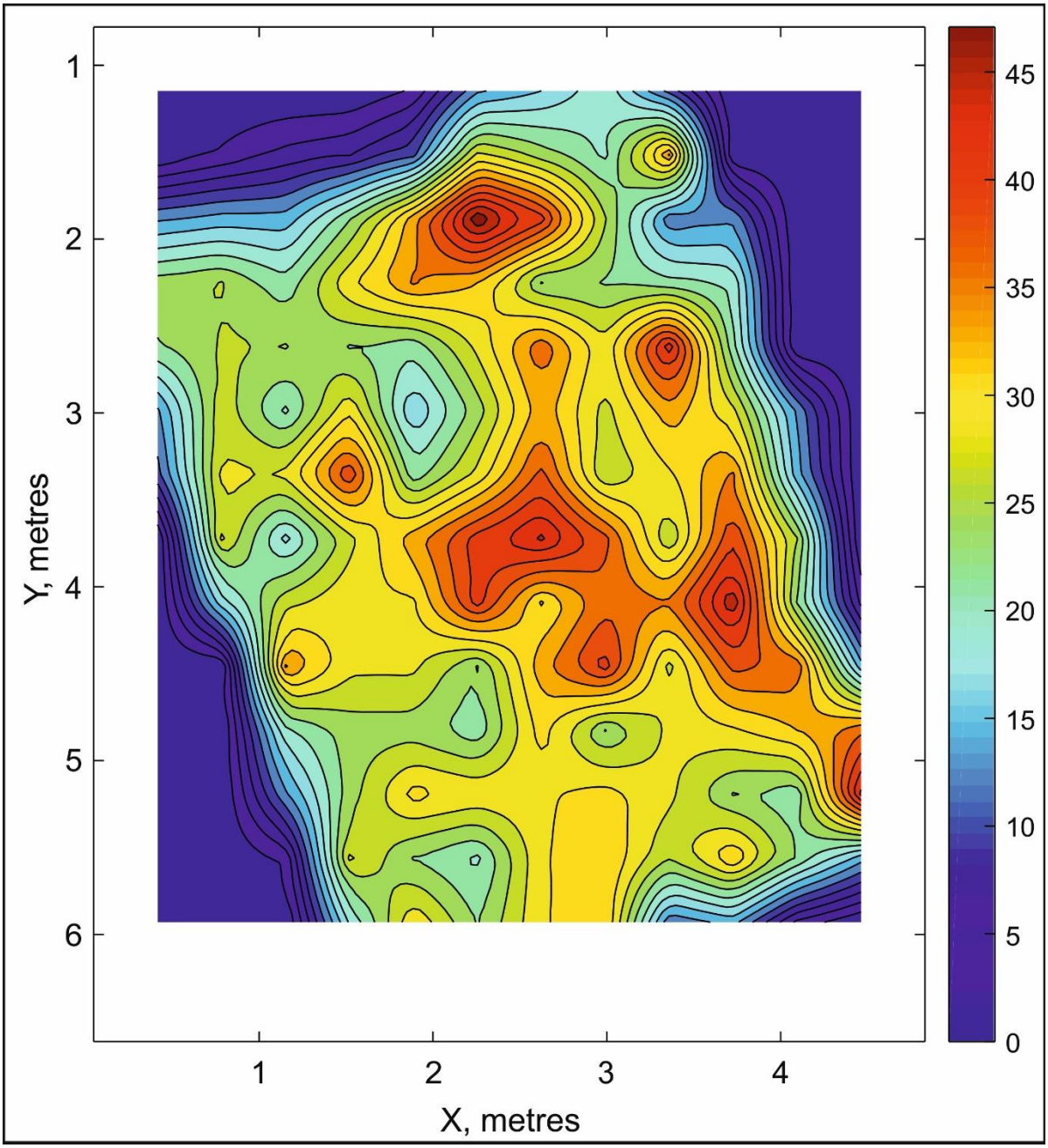

Fig 4.10: A fracture intensity (P_{21}) contour diagram of the Northern outcrop near Petakonkuppe, showing clusters of quite high values around 35-45 metre^{-1}(orange-red areas).

4.3.2 Southern sector

A procedure similar to that followed for the Northern outcrops was adopted for the South. One such representative outcrop was present near the road towards Talya.

Fig 4.11 shows the rose diagram of the fracture trace orientations as observed in the outcrop. Here, contrary to CDGN, the majority of fracture traces show a NE-SW orientation, along with a considerable increase in the diversity of orientations, compared to the North. The number of fracture segments measured, 17116, were significantly lower than the North, considering that the area of the measured outcrops were similar, if not equal.

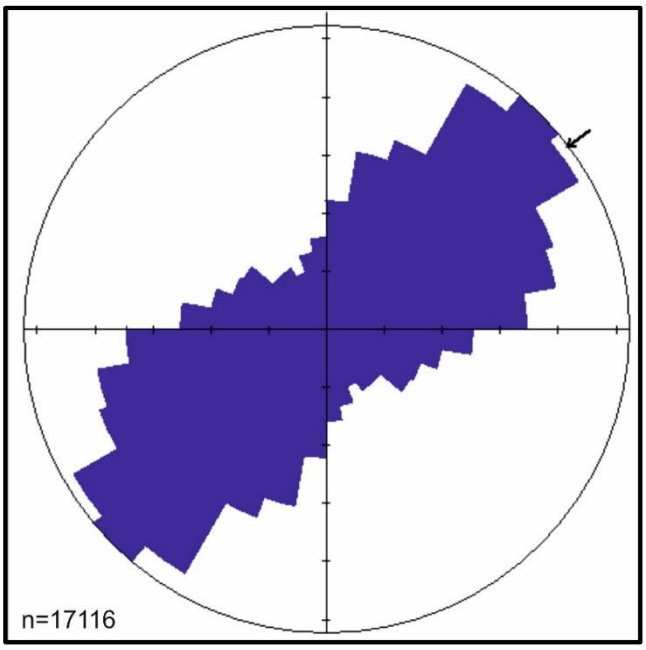

Fig 4.11: Rose diagram showing the major NE-SW orientation of fractures traced from the digital image. See Fig 4.12 for the traced outcrop.

Fig 4.12 shows us no distinct clustering pattern in the orientation trend of the fracture traces lengths, which was present in the North. The interpretations would be provided in the following chapter.

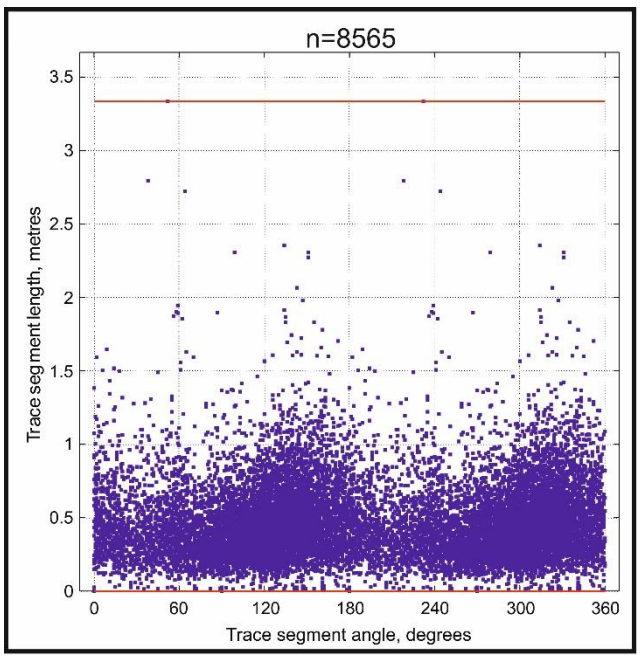

Fig 4.12: A plot of fracture trace segment length vs. their orientation, showing no major trends of the fracture traces. The red line demarcates maximum trace length.

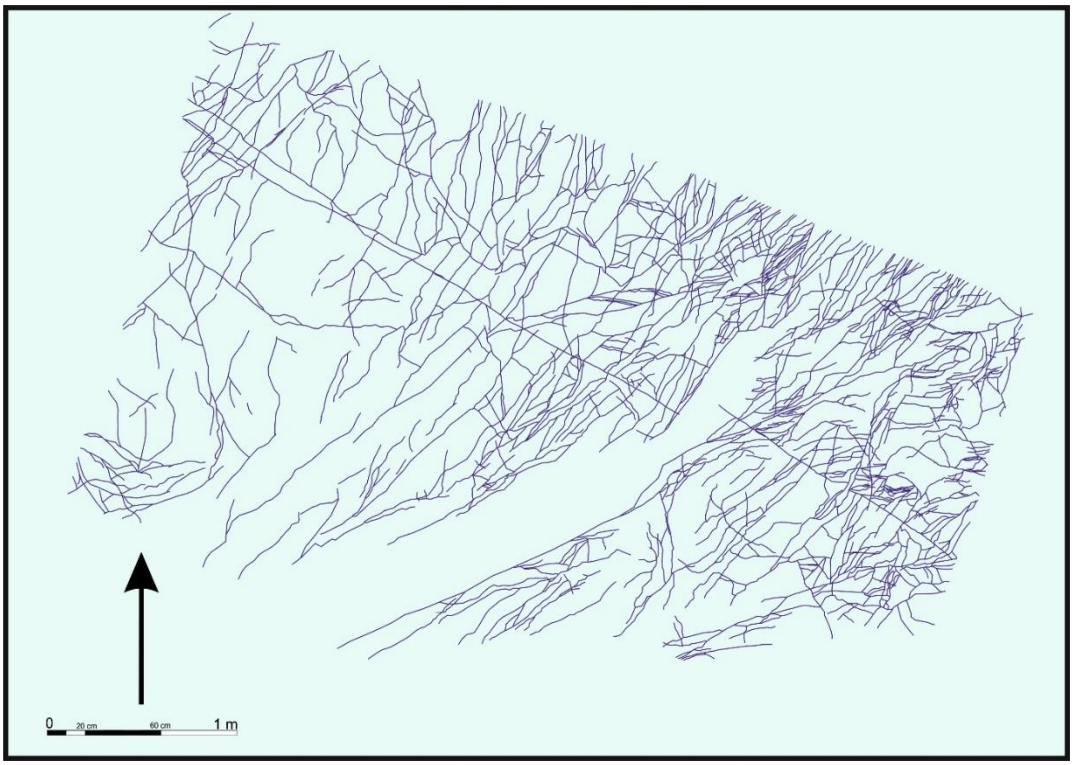

Fig 4.13: The digital fracture trace of the entire stitched outcrop of CDGS (near Talya), which was used as the input file for FracPaQ analysis, in an 8-bit binary image format.

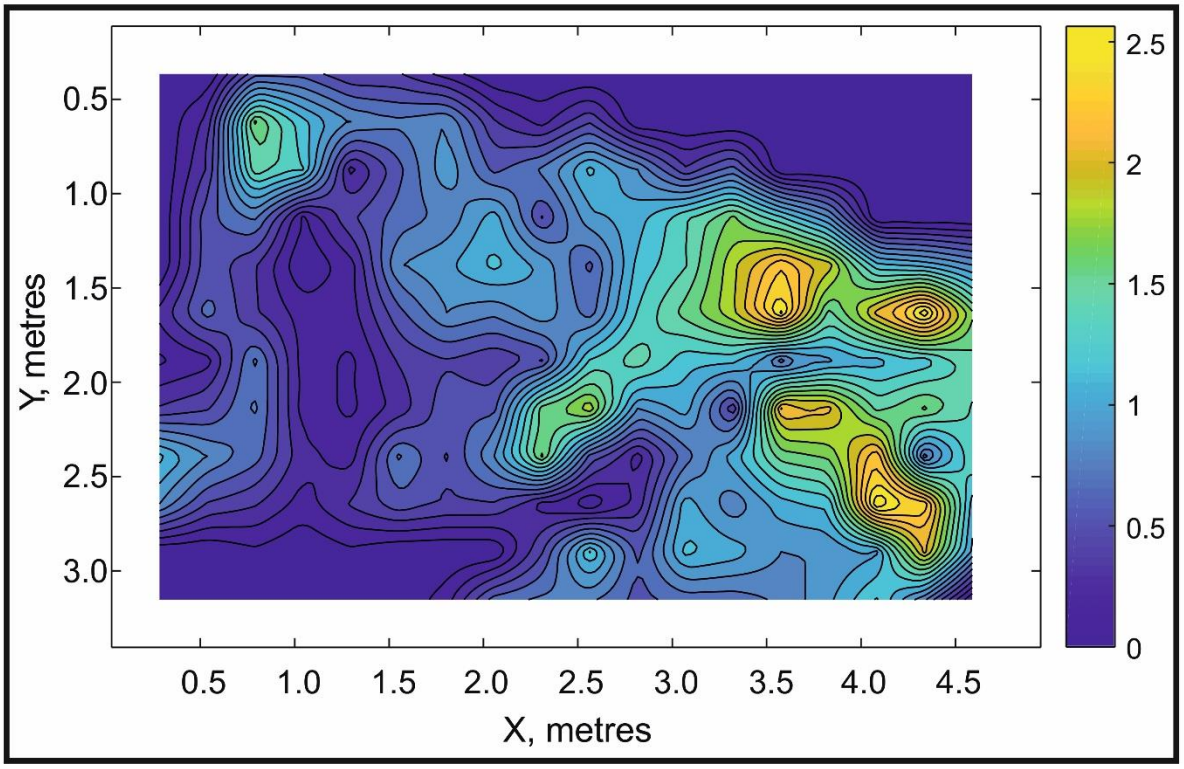

Fig 4.14: A fracture intensity (P_{21}) contour diagram of the Southern outcrop near Talya, showing clusters of quite low-moderate values around 2.5 metre^{-1}(yellow areas)

Fig 4.14 shows the fracture intensity map (P_{21}), of the traced outcrop (Fig 4.13), showing a few clusters with low values around 2.5 metre^{-1} (See section 3.5 for details). This contradicts the Northern observation where an almost equal area hosts a higher intensity of brittle fractures.

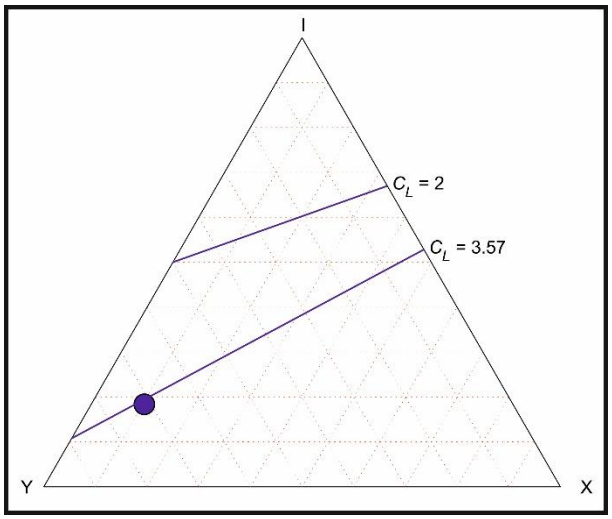

Fig 4.15: I-Y-X ternary diagram, obtained from FracPaQ, with the point showing the proportion of respective nodes in the Southern outcrop.

Fig 4.15 shows the I-Y-X ternary diagram (for more details see section 3.4), demarcating the position of the proportion of I, Y and X nodes as calculated from the CDGS outcrop. It can be seen that C_L shows a value beyond 3.57, indicating a greater proportion of Y-nodes than the North. The details will be dealt with in the following chapter.

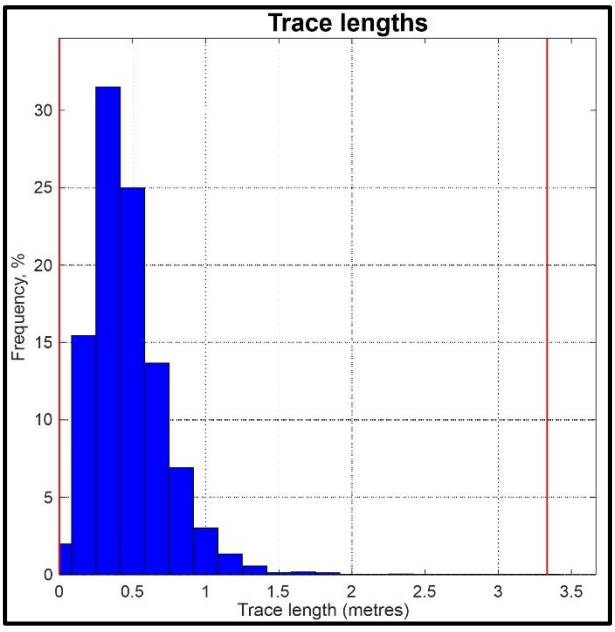

Fig 4.16: Histogram of the fracture trace length the Southern outcrop.

Fig 4.16 shows the histogram of fracture trace lengths, showing a higher distribution of individual fractures than the Northern counterpart, the maximum frequency being around 0.4 – 0.5 m, with the maximum trace length reaching more than 2 m.

The interpretations have been provided in the following chapter.

4.4 Statistical results

From the initial digital analysis using FracPaQ package, some primary data were obtained pertaining to the topological features of the respective outcrops. These were further used to calculate the number of branches, number of lines, ratio of branches to lines, connectivity coefficients and dimensionless intensity parameter for the respective sectors, using methods enumerated in Chapter 3, sections 3.3 and 3.5.

Variable	Description	Northern values	Southern values
N_I	No. of I-nodes	6339	1640
N_Y	No. of Y-nodes	13371	7290
N_X	No. of X-nodes	2527	1045
N_L	No. of lines	10005	4465
N_B	No. of branches	28730	13845
N_B / N_L	Branching ratio	**2.87**	**3.10**
C_B	Avg. no. of connections per branch	1.78	1.88
C_L	Avg. no. of connections per line	3.23	3.73
P_{20} (m^{-2})	Fracture density	616.9515	606.3916
P_{21} (m^{-1})	Fracture intensity	17.1385	12.2212
P_{22}	Dimensionless intensity	**0.47**	**0.24**

Table 4.1: List of secondary statistical values calculated from the topology of the fracture networks

So this chapter saw the enlistment of the results of each stage of data acquisition and topological analysis. The interpretation of these results in light of regional tectonics are provided in the following and final chapter.

CHAPTER 5

Discussion and Conclusions

5.1 Introduction

This present thesis has been aimed at understanding the prospective role of network topology in comprehending the fracture network in Chitradurga granite (Western Dharwar Craton, South India). The previous chapters have explained the regional setting on Chitradurga granite, the purpose behind studying such fractured granitoid plutons, the science behind the application of topology to study fracture networks in two dimensions, followed by the application and results. In this chapter, the discussions obtained from the present study along with possible conclusions followed by scope for future work are presented.

5.2 Temporal relationship between fracturing and regional deformation

It is mentioned earlier that the area has undergone three phases of deformation where D1/D2 deformation were coaxial on account of NE-SW compression and D3 was on account of WNW-ESE compression. This, in addition to the fact that the Northern and Southern portions are dominantly simple and pure sheared respectively (Mondal, 2018), has influenced the growth of tectonic fractures in Chitradurga granite. Furthermore, the presence of pre-existing thermal fractures (Fig 4.1, Fig 4.3), as distinguished by Mondal and Acharyya (2018), has also helped to shape the ultimate fracture network.

The sectors of the study area were chosen while keeping two factors in mind, namely, the difference in major fracture trace orientation and the difference in spatial distance of the two sectors from the eastward Chitradurga Shear Zone (CSZ). Here, it must be kept in mind that the presently observed fracture network is the result of deformation arising due to thermal and tectonic stresses. The first striking difference which can be observed is the major contrast in fracture trace orientation between the Northern and Southern outcrops, as shown in Fig 4.5 (North) and Fig 4.11 (South). It is normally expected that both sectors would show similar tectonic fracture orientations, since these fractures are found on the same granitic pluton and same state of stress.

The Northern outcrop shows a predominant NNW-SSE trend, albeit accompanied by a considerable orientation diversity. On the contrary, the Southern outcrop shows a predominant NE-SW trend, along with a greater diversity in fracture trace orientations. It could be possibly

explained by the effect of the late-stage brittle deformation event D3 on the Northern and Southern parts. The Northern sector is dominantly simple sheared (during D3), possibly leading to the formation of shear fractures (Fig 4.4 a, c) as well as leading to offset along pre-existing fractures (Fig 4.4 e). The spatial proximity to the CSZ accompanied by the dominant simple shearing probably exerted a greater control on the fracture orientation than the South, which is also evident in Fig 4.6, where fracture orientation clusters can be clearly distinguished. Thus these resulted in a lesser spread in the fracture orientation rose plot.

The Southern outcrop is dominantly pure sheared and it is situated farther away from the CSZ, contrary to the North. Probably, the majority of the fractures here are thermal in origin, due to the rarity of tectonic fractures (due to lesser control on fracture orientation), and due to spatial distance from CSZ. Due to greater diversity in the orientation of thermal fractures, the rose diagram shows greater orientation variation. The pluton shape has also influenced the spatial distance of Southern sector from the CSZ, contributing to the rarity of tectonic fractures. Hence the Southern sector shows a predominant NE-SW trend, with a greater orientation diversity, owing to the lack of an empirical controlling mechanism.

5.3 Network topology vis-à-vis regional deformation

The primary data regarding network topological analysis of the fracture networks concerns the different type of node counts (Table 4.1). Comparing the numbers, it is quite clear that CDGN has a greater number of fractures in the outcrop than CDGS. This points to a greater intensity of fracturing, resulting from factors mentioned in the previous section. From Fig 4.7 and Fig

4.15, it is evident that the proportion of Y-nodes has increased for the Southern outcrop. At the same time, the total number of fracture lines has decreased for the South (Table 4.1). On top of this, a comparison of Fig 4.8 and Fig 4.16 reveals that the fracture trace length is significantly higher for the South, with respect to the North. This indicates a greater tendency of fracture abutment on pre-existing fractures. The higher value of branching ratio (N_B / N_L) shown for the South (Fig 5.1) in Table 4.1 also indicates more number of branches existing per fracture trace, pointing to an abutting arrangement. Such a phenomenon will accumulate into a greater variation in the fracture orientation, as has been observed in Fig 4.11. Hence the topological results support the primary observations.

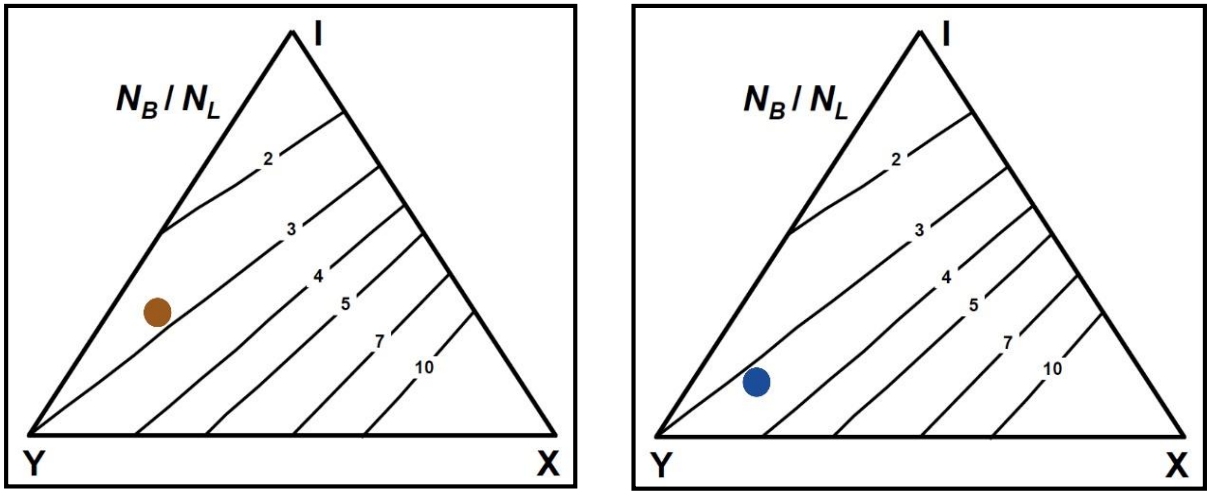

Fig 5.1: I-Y-X ternary diagrams of Northern (left) and Southern (right) outcrops showing respective values of branching ratio.

The previous section points out that the mechanism of fracturing and its control on fracture orientation is more effective in the Northern sector. If such is the case, then it should be reflected in the topological results as well. The dimensionless intensity P_{22}, calculated from the

outcrop network topology is almost twice as high in the North compared to the South (Table 4.1). These values can be extrapolated for the entire pluton due to the scale independence feature. This supports the above preliminary assumption.

The effect of fracture network pattern on its connectivity is evident while comparing the values of connectivity coefficients C_B and C_L (Table 4.1). The greater the diversity in fracture orientation in a network, the greater should be its connectivity. This is clearly reflected in the higher values of the aforementioned variables for the Southern outcrop. So, once more, topology confirms the initial conjecture. It further stresses on the point that the fracture orientation variation is a more dominant contributor to connectivity than fracture intensity, since connectivity for the more intensely fractured CDGN is lesser than the more diversely oriented fractures of CDGS.

5.4 Conclusion

Topology essentially describes the relationship between fractures in a network. In this study, fracture networks from two dimensional horizontal outcrops of Chitradurga granite (WDC, South India) were studied with the help of network topology. The obtained results in the previous chapter and their interpretation with regard to regional deformation enables the possibility of using topology as a standard tool in fracture network characterization, free from any observer-based bias.

- Node counting and branch analysis helped to determine the orientation, frequency and intensity of fractures
- The proportions of different types of nodes provided a basis for describing the topology that can be easily applied even with limited access to the network as a whole
- Plots of the proportions of I-, Y- and X-nodes provided a simple summary of some aspects of the topology and are useful in distinguishing different networks. The plot describes topology rather than geometry since it is unchanged by any continuous transformation of the network
- Node counting provided an unbiased estimate of frequency and was used in conjunction with fracture intensity to estimate the characteristic length (L_C) and dimensionless intensity (P_{22}) of the fractures.
- This provided a measure of fracture development that is independent of scale and can be extrapolated to serve many practical applications.
- Determining both the geometry and topology of fractures allowed us to improve the characterization of fracture networks, both in terms of the efficiency of the methodology and the range of derived parameters.
- The interpretations obtained with topological analysis corresponded well with the observed and previously established results.

5.5 Scope for future work

This study has given a primary demonstration of the use of topology as a tool to deconstruct and characterize the fracture networks of Chitradurga granite. Certain aspects of Chitradurga, which, if investigated further, might yield more interesting revelations about fracture formation and interaction during the entire deformation history of CDG.

- The present analysis deals with only two sectors, at the Northern and Southern ends. Further research must be conducted throughout the entire pluton to find out the transitional topological characteristics of the existing fracture network
- Emphasis must be laid on the extrapolation of topological studies to three dimensions, using well or borehole data
- Microstructural analysis could be conducted to determine fractal dimensions of the fracture network
- Further research needs to be conducted to evaluate the hydrodynamic consequences of the fracture network, in order to categorize its potential as a nuclear waste storage site.
- Extrapolation of topological analysis to other adjacent rocks (vein-hosting metabasalt) to aid in fluid flow and permeability studies.

REFERENCES

Acharyya, S. S., & Mondal, T. K. (2019). Stress enhanced tensile fractures in elliptical clast in conglomerate. *Journal of Structural Geology*, *122*, 81-88.

Atkinson, B.K., Meredith, P.G., (1989). Experimental fracture mechanics data for rocks and minerals. In: Atikinson, B.K. (Ed.), Fracture Mechanics of Rocks. Academic Press, London, pp. 477–525.

Balakrishnan, S., Hanson, G. N., Rajamani, V., (1999). U–Pb ages for zircon and titanite from the Ramagiri area, southern India: evidence for accretionary origin of the Eastern Dharwar Craton during the late Archean. Journal of Geology 107, 69–86.

Beeraiah, M. B., Ananthanarayana, R., Khan, R., Sengupta, S., Ramesh, N. R., Rao, K. B., Narasimha, S., Ramachandran, T. V., (1998). A report on the specialised thematic mapping and geochemical surveys in Gadag schist belt, Dharwar district, Karnataka. Progress report for the field season 1993–95.

Bhaskar Rao, Y. J., Naha, K., Srinivasan, R., Gopalan, K., (1991). Geology, geochemistry and geochronology of the Archaean Peninsular Gneiss around Gorur, Hassan District, Karnataka, India. Indian Academy of Science (Earth and Planetary Sciences) Proceedings 100, 399–412.

Bhatt, S., Rana, V., & Mamtani, M. A. (2017). Deciphering relative timing of fabric development in granitoids with similar absolute ages based on AMS study (Dharwar Craton, South India). Journal of Structural Geology, 94, 32-46.

Chadwick, B., Ramakrishnan, M., Vasudev, V. N., Viswanatha, M. N., (1989). Facies Distributions and Structure of a Dharwar Volcanosedimentary Basin: Evidence for Late Archaean transpression in Southern India? Journal of the Geological Society of London 146, 825–834.

Chadwick, B., Ramakrishnan, M., and Viswanatha, M, N., (1981). The stratigraphy and structure if the Chitradurga region: an illustration of cover-basement interaction in the late Archaean evolution of the Karnataka craton, southern India: Precambrian Research, v. 16, p. 31-54.

Chadwick, B., Vasudev, V.N., and Hedge, G.V., (2003), The Chitradurga schist belt and its adjacent plutonic rocks NW of Tungabhadra, Karnataka: a duplex in the late Archean convergent setting of the Dharwar craton: Journal of Geological Society of India, v. 61, p.611-613.

Chatterjee, A. P., & Mondal, T. K. (2018, December). Fracture network characterization in syn-tectonic granite: an example from Chitradurga Schist Belt, Dharwar craton, south India. In AGU Fall Meeting Abstracts.

Chakrabarti, C., Mallick, B. S., Pyne, T. K., Guha, D., (2006). A manual of the Geology of India. Geological Survey of India, Kolkata.

Dershowitz, W. S., & Einstein, H. H. (1988). Characterizing rock joint geometry with joint system models. Rock mechanics and rock engineering, 21(1), 21-51.

Dershowitz, W. S., & Herda, H. H. (1992, January). Interpretation of fracture spacing and intensity. In The 33th US Symposium on Rock Mechanics (USRMS). American Rock Mechanics Association.

Fossen, H., (2011). Structural Geology. Cambridge University Press.

Healy, D., Rizzo R.E., Cornwell D. G., Farrell N. JC, Watkins H., Timms N. E., Gomez-Rivas E., and Smith M.. "FracPaQ: A MATLAB™ toolbox for the quantification of fracture patterns." Journal of Structural Geology 95 (2017): 1-16.

Holcombe, R., (2003). GEOrient.

Jaeger, J.C., Crook, N.G.W., Zimmerman, R.W., (2007). Fundamentals of Rock Mechanics. Blackwell Publishing Ltd

Jayananda, M., Chardon, D., Peucat, J. J., & Capdevila, R. (2006). 2.61 Ga potassic granites and crustal reworking in the western Dharwar craton, southern India: tectonic, geochronologic and geochemical constraints. Precambrian Research, 150(1-2), 1-26.

Jayananda, M., Peucat, J.-J., Chardon, D., Krishna Rao, B., Fanning, M. C., Corfu, F., (2013). Neoarchean greenstone volcanism and continental growth, Dharwar craton, south India: constraints from SIMS U–Pb zircon geochronology and Nd isotopes. Precambrian Research 227, 55–76.

Jing, L., & Stephansson, O. (1997). Network topology and homogenization of fractured rocks. In Fluid flow and transport in rocks (pp. 191-202). Springer, Dordrecht.

Manikyamba, C., Naqvi, S. M., Subba Rao, D. V., Ram Mohan, M., Khanna, T. C., Rao, T. G., Reddy, G. L. N., (2005). Boninites from the Neoarchaean Gadwal Greenstone belt, Eastern Dharwar Craton, India: implications for Archaean subduction processes. Earth and Planetary Science Letters 230, 65-83.

Manzocchi, T. (2002). The connectivity of two-dimensional networks of spatially correlated fractures. Water Resources Research, 38(9).

Meert, J.G., Pandit, M.K., Pradhan, V.R., Banks, J., Sirianni, R., Stroud, M., Newstead, B. and Gifford, J., (2010). Precambrian crustal evolution of Peninsular India: a 3.0 billion year odyssey. Journal of Asian Earth Sciences, 39(6), pp.483-515.

Mondal, T.K. and Mamtani, M.A., (2016). Palaeostress analysis of normal faults in granite–implications for interpreting Riedel shearing related to regional deformation. Journal of the Geological Society, 173(1), pp.216-227

Mondal, T. K. (2018). Evolution of fabric in Chitradurga granite (south India)-A study based on microstructure, anisotropy of magnetic susceptibility (AMS) and vorticity analysis. Tectonophysics, 723, 149-161.

Mondal, T. K., & Acharyya, S. S. (2018). Fractured micro-granitoid enclaves: A stress marker. Journal of Structural Geology, 113, 33-41.

Morley, C.K. and Nixon, C.W., (2016). Topological characteristics of simple and complex normal fault networks. Journal of Structural Geology, 84, pp.68-84.

Naha, K., Srinivasan, R., Jayaram, S., (1991). Sedimentological, structural and migmatitic history of the Archaean Dharwar tectonic province, southern India. Proceedings of the Indian Academy of Science (Earth Planetary Science) 100, 413–433.

Naqvi, S. M., & Rogers, J. J. W. (1987). Precambrian geology of India. Oxford University Press.

Nixon, Casey (2013), Analysis of fault networks and conjugate systems, University of Southampton, Faculty of Natural and Environmental Sciences, Ocean and Earth Sciences, PhD Thesis.

Nixon, C. W., Sanderson, D. J., & Bull, J. M. (2012). Analysis of a strike-slip fault network using high resolution multibeam bathymetry, offshore NW Devon UK. Tectonophysics, 541, 69-80.

Peacock, D. C. P., Nixon, C. W., Rotevatn, A., Sanderson, D. J., & Zuluaga, L. F. (2016). Glossary of fault and other fracture networks. *Journal of Structural Geology*, *92*, 12-29.

Peacock, D. C. P., Nixon, C. W., Rotevatn, A., Sanderson, D. J., & Zuluaga, L. F. (2017). Interacting faults. *Journal of Structural Geology*, *97*, 1-22.

Peacock, D. C. P., Sanderson, D. J., & Rotevatn, A. (2018). Relationships between fractures. Journal of Structural Geology, 106, 41-53.

Peacock, D. C. P., & Sanderson, D. J. (2018). Structural analyses and fracture network characterisation: Seven pillars of wisdom. Earth-Science Reviews.

Pitchamuthu, C. S., Srinivasan, R., (1984). The Dharwar Craton. Perspective Report Series, 7, Indian National Science Academy, 3–34.

Plavsa, D., Collins, A. S., Foden, J. F., Kropinski, L., Santosh, M., Chetty, T. R. K., Clark, C., 2012. Delineating crustal domains in Peninsular India: age and chemistry of orthopyroxene–bearing felsic gneisses in the Madurai Block. Precambrian Research 198–199, 77–93.

Ramakrishnan M., Vaidyanadhan R., & Geological Society of India. (2008). Geology of India (Vol. 1). Geological Society of India.

Ramsay, J. G., Lisle, R. J., (2000). The Techniques of Modern Structural Geology. Vol. 3: Applications of Continuum Mechanics in Structural Geology. Academic Press, London.

Rogers, J. J. (1986). The Dharwar craton and the assembly of peninsular India. The Journal of Geology, 94(2), 129-143.

Rollinson, H. R., Windley, B. F., Ramakrishnan, M., (1981). Contrasting high and intermediate pressures of metamorphism in the Archaean Sargur Schists of southern India. Contributions to Mineralogy and Petrology 76, 420–429.

Sanderson, D. J., & Nixon, C. W. (2015). The use of topology in fracture network characterization. Journal of Structural Geology, 72, 55-66.

Sanderson, D. J., & Nixon, C. W. (2018). Topology, connectivity and percolation in fracture networks. Journal of Structural Geology, 115, 167-177.

Segall, P, and Pollard, D. D., (1983), Nucleation and growth of strike slip faults in granite: Journal of Geophysical Research, v. 88(b1), p.555-568.

Sengupta, S., Roy, A., (2012). Tectonic Amalgamation of Crustal Blocks along Gadag Mandya Shear Zone in Dharwar Craton of Southern India. Journal of the Geological Society of India 80, 75–88.

Sharma, R. S. (2009). Cratons of the Indian shield. In Cratons and fold belts of India (pp. 41-115). Springer, Berlin, Heidelberg.

Taylor, P. N., Chadwick, B., Moorbath, S., Ramakrishnan, M., & Viswanatha, M. N. (1984). Petrography, chemistry and isotopic ages of Peninsular Gneiss, Dharwar acid volcanic rocks and the Chitradurga granite with special reference to the late Archean evolution of the Karnataka craton, Southern India. Precambrian Research, 23(3-4), 349-375.

Valdiya, K. S. (2010). The making of India-Geodynamic evolution. Macmillan Pub. India. Ltd.